Aalto University
School of Science

Master's Programme in Mathematics and Operations Research

A biobjective mixed-integer linear program for decarbonized bunkering locations in the Baltic sea.

Mattias Österbacka

Master's Thesis
2024

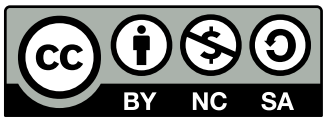

Aalto University
School of Science

Author Mattias Österbacka

Title A biobjective mixed-integer linear program for decarbonized bunkering locations in the Baltic sea.

Degree programme Mathematics and Operations Research

Major Systems and Operations Research

Supervisor Asst. Prof. Philine Schiewe

Advisors DSc. (tech) Markus Rautanen, Lic. (tech) Robert Weiss

Collaborative partner Technical research centre of Finland, VTT

Date September 23, 2024 **Number of pages** 63+9 **Language** English

Abstract

Maritime shipping accounts for almost 3% of yearly global greenhouse gas emissions. One potential way to reduce these emissions is to switch from burning oil to renewable synthetic fuels. Hydrogen and ammonia can be produced in a renewable way, and can be fed into a fuel cell to directly generate electricity to power a ship. Ammonia can also be burned in engines like traditional marine fuels, aiding the potential switch. In this thesis, a biobjective mixed-integer linear program is developed and implemented to aid in optimally placing renewable bunkering locations in the Baltic Sea. A price model for producing hydrogen and ammonia around the Baltic Sea, as well as historical ship data is used in conjunction with the optimization model. Several solution approaches for multiobjective optimization problems are implemented and used to compute Pareto optimal solutions. A robustness measure for production locations, called the core index, is applied. Based on the robustness measure, we identify ports where producing renewable bunkering fuel is advisable, even if the preference between reducing emissions and keeping costs down is not known in advance. Sensitivity analysis is performed to gauge how the results are impacted by changes in input parameters.

Keywords MILP, Optimization, Bunkering location, Baltic Sea, Core index, Hydrogen, Ammonia

Aalto-universitetet
Högskolan för
teknikvetenskaper

Författare Mattias Österbacka

Titel Ett flermåls blandat heltalsprogram för avkarboniserade bunkringsplatser i Östersjön.

Utbildningsprogram Mathematics and Operations Research

Huvudämne Systems and Operations Research

Övervakare Biträdande professor Philine Schiewe

Handledare Teknologie doktor Markus Rautanen, Teknologie licentiat Robert Weiss

Samarbetspartner Teknologiska forskningscentralen VTT

Datum 23 september 2024 **Sidantal** 63+9 **Språk** engelska

Sammandrag

Maritim sjöfart står för nästan 3% av globala växthusgasutsläpp årligen. Detta är ett faktum som måste åtgärdas. Ett sätt att minska på utsläppen från sjöfarten är att byta ut de traditionella oljebaserade bränslena, mot nya syntetiska förnybara bränslen. Exempel på sådana med hög potential är väte och ammoniak. Dessa kan produceras rakt med elektricitet, och kan matas in i en bränslecell för att generera elektricitet ombord på ett skepp. Ammoniak kan också användas rakt i en traditionell förbränningsmotor.

I detta diplomarbete har en flermåls heltalsoptimeringsmodell utvecklats och implementerats för att understöda optimal placering av förnybara bunkringsplatser i Östersjön. I arbetet antas det att om väte eller ammoniak behövs för bunkring i en hamn måste det produceras lokalt. Till skillnad från väte, så kan ammoniak även köpas från marknaden, eftersom det existerar en marknad för förnybar ammoniak. Till detta har också en prismodell för väte och ammoniak i de olika länderna runt Östersjön utvecklats. Optimeringsmodellen har körts på historiskt sjöfartsdata från år 2023. Denna data består av rutter mellan olika hamnar för olika skeppstyper. Utöver detta har olika flermåls problemlösare testats. En robusthetsmetrik för hamnar, kallat kärnindex, är introducerat. Ett högt kärnindex för en hamn betyder att det med hög sannolikhet är lönt att producera syntetiska bränslen i denna hamn.

Med hjälp av dessa verktyg kan hamnar, där det är optimalt att producera syntetiska bränslen för bunkring, identifieras. Olika lösningar med olika kostnader presenterades. Kärnindexet användes också för att kategorisera olika hamnar. De hamnar med det högsta kärnindexet, dvs där det är högst sannolikt lönt att producera syntetiska bränslen för bunkring, är Göteborg, Sverige; Åbo, Finland; Kotka, Finland; Helsingfors, Finland och Gävle, Sverige. Dessa hamnar är optimala på grund av en kombination av vätgaspriset och mängden skeppstrafik.

En detaljerad känslighetsanalys gjordes, både på syntetiska bränslepriset, och på parametern för minimiproduktionstakten. Som följd av analysen identifierades vissa hamnar som eventuellt optimala om några av dessa storheter ändrades lite, och andra som inte känsliga till förändringar, dvs. hamnarna fortsätter vara optimala eller icke optimala.

Nyckelord Optimering, bunkringsplats, Östersjön, heltalsprogrammering, kärnindex, vätgas, ammoniak

Preface

I want to thank my thesis supervisor Philine Schiewe and my advisors Markus Rautanen and Robert Weiss for their excellent guidance and willingness to discuss any problems that did arise. I want to thank my colleagues at VTT for keeping the spirits high at the office. Finally I want to thank my friends, family, and especially partner for guiding me through this important part of my life.

Otnäs, 26 September 2024

Mattias Österbacka

Contents

Symbols and abbreviations

Symbols

$\mathbb{N}$	the set of natural numbers, 0 included
$\mathbb{R}$	the set of real numbers

Abbreviations

DM	decision maker
EU	European Union
GHG	greenhouse gases
g_{CO2eq}	grams of CO_2 equivalent emissions
HFO	heavy fuel oil
ICE	internal combustion engine
IMO	International Maritime Organization
LNG	liquefied natural gas
LP	linear program
MDO	marine diesel oil
MILP	mixed-integer linear program
min.	minimize
NOx	nitrogen oxides
PM10	particulate matter
PPA	power purchase agreement
s.t.	subject to
SOx	sulphur oxides
Synfuel	synthetic fuel
TTW	tank-to-wake

1 Introduction

A study done by the International Maritime Organization (IMO) claims that green house gases (GHG) from the shipping industry has increased by 9.6% from 2012 to 2018 [1]. During the same time, the share of total global emissions from the shipping industry has increased from 2.76% to 2.89%. This has happened while the carbon intensity of ships, on average, has actually decreased by 21-31% depending on the metric used. However, this decrease in carbon intensity has slowed down in recent years. Total emissions from shipping is currently predicted to continue to rise until 2050. Thus there is an urgent need to lower the GHG emissions from shipping, and IMO has developed a plan to reduce the amount of GHG emissions from shipping by at least 70% by 2040 [2].

Emission free fuels need to be implemented and deployed in the shipping industry to reach decarbonisation goals by 2050 [3]. To reach decarbonisation, different ways of managing demand, such as logistic optimization and curtailing traffic volumes have been explored. Adding to this, an improvement in ship design and propulsion technology could possibly reduce the GHG emissions by up to 55%. This, however, is not enough, thus we need marine fuels that are emission free to meet the goals set up by IMO.

Mathematical optimization has widely been used within the maritime shipping industry [4]. Problems that require decision making quickly become very large when dealing with large shipping networks, different ports, and different requirement from different actors within shipping.

In this thesis, we develop a multi-objective optimization model, to model where in the Baltic sea decarbonised bunkering solutions for maritime shipping could be be optimally placed. In this context bunkering means refueling for ships, and bunker fuel is ship fuel. This model is then solved using real world voyage data from shipping in the Baltic sea. The purpose of this model is to aid the uptake of decarbonised, emission free fueling for ships.

2 Background

This section first presents the current situation regarding emissions in the shipping industry. Then synthetic fuels, hydrogen and ammonia are presented. Mathematical optimization has been used a lot in the shipping industry and is then presented. Finally, we go more in depth into the mathematical side of optimization.

2.1 Emissions in shipping

Maritime shipping is the most energy efficient mode of transportation we currently have [4]. A modern container ship is much more efficient than trains, trucks, or planes, as shown in Figure 1. Thus, around 80% of world trade is done through maritime shipping.

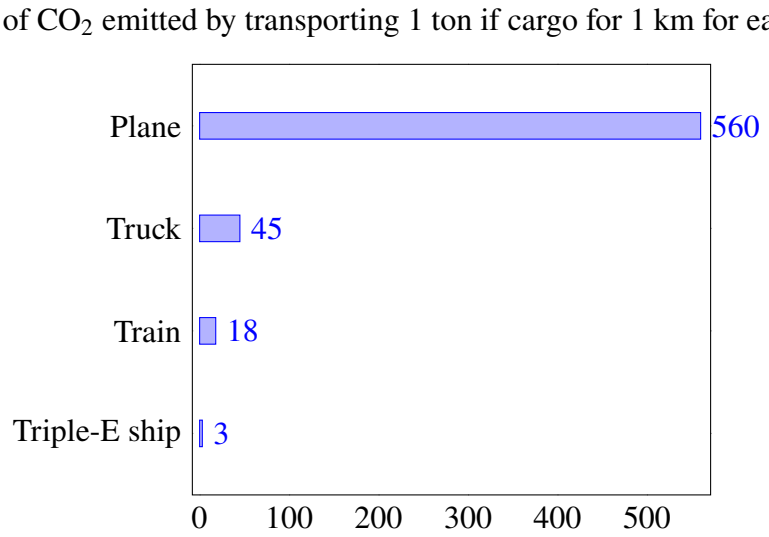

Figure 1: Shipping type emission data from [4]. A Triple-E ship is a specific type of large container ship.

As previously mentioned, total GHG emissions from shipping is still rising [1]. The demand for shipping is also continuing to rise which places an even higher demand on reducing GHG emissions [5]. The development of maritime GHG emissions since the 1990s can be divided into three periods. Figure 2 shows this phenomenon. The solid orange line shows the global maritime shipping demand, and the blue line shows GHG emissions emitted by maritime shipping. Before 2008, demand and emissions increased linearly together. After 2008 followed a short period of carbon emission reduction, while shipping demand continued to increase, but at a slower rate than before 2008. Finally, after 2014, GHG emissions have risen slowly again, while shipping demand continues to rise as fast as before 2008.

The marine fuel that is most commonly used today is heavy fuel oil (HFO), accounting for a 79% share of fuel consumption [5]. The second and third most used marine fuels are marine diesel oil (MDO) and liquefied natural gas (LNG),

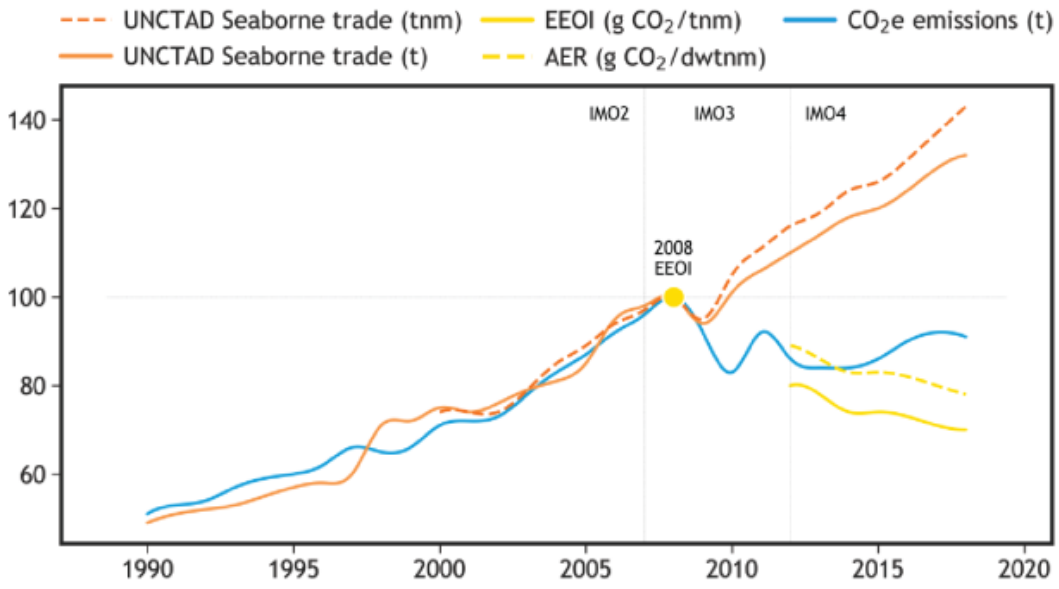

Figure 2: Global shipping emissions and trade demand, acquired from the Fourth IMO GHG Study 2020 executive summary [5].

respectively. Looking at ship types, bulk carriers, container ships, and oil tankers consume by far the most fuel [5]. Trailing behind are chemical tankers, general cargo ships, and liquefied gas tankers. Ships usually need fuel for several purposes, such as propulsion, auxiliary engines, and boilers. Here, propulsion is by far the largest consumer of fuel.

Not only does the shipping industry release large amounts of GHG emissions, air pollutants are also released [6]. This is partly due to HFO being essentially a byproduct of oil refining, so it is impure [7]. The worst of these pollutants are sulphur oxides (SOx), nitrogen oxides (NOx), and particulate matters (PM10) [6]. Not only do these pollutants contribute to climate change, but unlike carbon dioxide, they impact the health of humans and the quality of air negatively.

It is clear that emissions from the shipping industry needs to be reduced. The International Maritime Organization (IMO) have developed a strategy to reach net-zero by 2050 [2]. This strategy includes steps, such as increasing the use of zero emission fuels, technologies, and energy sources to at least 5% by 2030. After that the ambition is to reach net-zero emissions by around 2050. This thesis is related to these two points, i.e., where is it optimal to place decarbonised bunkering (i.e. refueling) stations for ships in the Baltic sea.

2.2 Synthetic fuels

Synthetic fuels or synfuels encompass more than the traditional definition of fuels made from syngas derived from coal, or hydrocarbons that are produced from sources other than petroleum [8]. The traditional hydrocarbon connection is narrow, but understandable given their heavy use in modern society. A more modern definition

that is more general places fuels on a spectrum such that they are primarily produced by hydrogen addition, carbon rearrangement, or usually a combination of both.

When considering synfuels, there are three criteria to take into consideration [8]. These are renewability, feasibility at scale, and usability in existing infrastructure. Regarding renewability, perhaps the most important factor is that any hydrogen feedstock used needs to be produced in a renewable fashion, i.e., via electrolysis. For scalability, the processes need to be able to be scaled up from laboratory test to large scales. E.g. Fischer-Tropsch synthesis producing liquid hydrocarbons has been demonstrated at an industrial scale. Finally, regarding suitability for existing infrastructure, e.g. renewable methane can be used in natural gas infrastructure, and liquid synfuels could be used in the transportation sector. Finally it is worth noting that a diverse portfolio of synfuels is needed to, e.g. minimize production uncertainties, instead of trying to focus on a single "best" fuel.

2.2.1 Hydrogen

One potential synthetic fuel that has been explored is hydrogen [9]. Hydrogen as a marine fuel offers many potential upsides. Fuel cells, which produce electricity directly from hydrogen, have higher efficiencies compared to internal combustion engines. Hydrogen is used as a feedstock for other potential synthetic fuels, such as ammonia and methanol, which means it is much less energy intensive to create hydrogen compared to other potential synfuels. Using hydrogen as a fuel only produces water as a byproduct, which means hydrogen is emission free, as long as it is also produced in such a way. There are however several downsides of using hydrogen as a marine fuel, it is much less volumetrically dense, potentially requiring up to seven times more space on a ship compared to traditional fuel oils [10]. This means that cargo carrying capacity can be negatively affected. Storage of the fuel onboard the ship is also much more difficult compared to fuel oils, as is refueling. Converting ships to use hydrogen as a fuel might also lead to ship operators being forced to bunker, i.e. refuel, more often [9].

As previously mentioned, to be able to use hydrogen as a emission free marine fuel, the hydrogen has to be produced in an emission free way [9]. Hydrogen can be categorised into gray, blue, and green hydrogen [11]. Gray hydrogen is the most common type of hydrogen produced today. It is produced from fossil sources, and as a byproduct, emits carbon dioxide. Blue hydrogen is very similar to gray, except the produced carbon dioxide is captured, and thus not emitted. Green hydrogen is, as the name implies, produced completely using renewable energy sources. The most promising green hydrogen technology is water electrolysis. Electrolysis works by splitting water into hydrogen and oxygen with electricity. This implies that the electricity used for electrolyzers must be renewable itself. Wind and solar seem to be the most promising candidates.

2.2.2 Ammonia

Another promising synthetic fuel candidate is ammonia [12]. Ammonia is an inorganic compound with the chemical formula NH_3. Ammonia can be used as a hydrogen carrier in fuel cells, or used straight in an internal combustion engine (ICE). Since ammonia is inorganic, burning it releases no carbon dioxide emissions. Ammonia has a relatively high volumetric energy density of 4.8 MWh/m^3 compared to 1.4 MWh/m^3 for hydrogen compressed to 700 bar [13]. Thus, ammonia has roughly half the volumetric energy density of HFO, which is at 9.7 MWh/m^3. Since ammonia is widely used in the fertilizer industry worldwide, there already exists infrastructure and regulations related to ammonia [12]. This means that a potential switch to ammonia for the shipping industry could be relatively easy. However, there are also downsides to ammonia, synthesizing ammonia through the Haber-Bosch process is very energy intensive [13]. Ammonia is also very toxic and corrosive. Furthermore, since ammonia contains nitrogen, burning it in an ICE releases NOx compounds [12]. In 2022 the first ever ammonia ready ship was delivered [14].

2.3 Mathematical optimization in the shipping industry

Due to the size and complexity of maritime shipping networks, optimization tools have been implemented for several purposes within the industry to achieve efficiency [4]. We can divide the problems into three different levels, strategic, tactical, and operational. The strategic problems include which markets to serve, fleet size and composition, as well as route design. Tactical problems include service selection, cargo routing, fleet deployment, speed optimization, and scheduling. Finally, operational problems include vessel berthing, container placement within the ship, empty container management, and disruption management.

To model these types of problems mathematically presents some difficulty regarding the uncertainty of the available data [4]. Demand from customers fluctuate throughout the year, weather can have a large impact on arrival times, and technical problems in ports can cause delays. Ports themselves also favour ships sticking to their original timetable, which makes changing the arrival times or the routes themselves difficult for ship operators.

The cost of fuel is the most important factor for the operating costs of a ship [15]. Up to 75% of the operating costs can stem from fuel costs. Thus, optimizing the sailing speed of a fleet can yield great monetary gains. Fuel consumption is often modeled by the speed of the vessel cubed [4]. However, in practice many factors impact fuel consumption such as vessel type, draught of the vessel, weather conditions, and more. A model to determine the optimal sailing speed and fleet size for a given set of port calls is presented in [15]. They also concluded that the optimal sailing speed is dependant on the current oil price.

Since most countries do not have a perfect trade balance, empty containers accumulate in import heavy regions [4]. These empty containers have to be repositioned by the shipping companies that own them, which can be very expensive. Thus, repositioning has to be handled in an optimal way. It is estimated that around 20% of

port activities are just for repositioning of empty containers [16]. Optimization has been used to save over $80 million for a large shipping company by reducing empty container inventory [17].

Determining the placement of the containers within the ship itself (stowage planning) is no trivial task [4]. Not only can modern ships carry large amounts of containers, the final list of goods is usually known very late, thus very fast algorithms are needed. First, factors such as weight, volume, and electrical outlets (usually for refrigerated containers), is needed to be considered when determining the mixture of containers. This is usually called the master planning problem. Second, the containers should be assigned so that loading and unloading time is minimized, and so that the ship is stable and not under too much mechanical stress. This is called the slot planning problem. Other factors to consider are that containers need to be loaded from the bottom up, the height of container stacks are limited by the line of sight from the bridge, the weight needs to be distributed evenly and below a set maximum limit, and that rearranging containers at each ports should be avoided. It is clear why stowage planning is so important. A model for the master planning problem is presented in [18]. The model considers several types of containers, and can be solved quickly for large ships.

While estimates vary, up to 75% of the operating costs of a ship can be attributed to bunkering fuel costs [19, 15]. Fuel prices are dependent with oil prices, and bunkering in some ports is more expensive than in others [4]. Thus, bunkering in an optimal way is important. The bunkering problem tries to minimize bunkering costs while assuring vessels have enough fuel. These problems can involve hundreds of vessels and thousands of port calls. A model presented in [20] maximizes profits for a ship operator company, while taking into account the uncertainty of bunkering costs using Markov processes. Markov processes are mathematical models used to model uncertainty, such as the uncertainty in bunker fuel prices.

Around 70% of shipping round trips are expected to experience delays in one or more ports [4]. Ship operators usually decide the course of action when a delay occurs manually. Delays can usually propagate due to the complexity of the shipping network, thus, handling delays in an optimal way is important. The vessel schedule recovery problem is presented in [21], which optimizes the trade off between the increased fuel consumption from speeding up vessels, and the impact the delays have on the cargo. The model demonstrated superior results compared to a trained professional, and savings up to 58% were observed.

This thesis can be considered related to the bunkering problem, since the optimization of bunkering is included. However, the problem presented in this thesis is novel in the sense that it is more a facility location problem with a heavy focus on reducing emissions in the shipping industry. We need to choose at which ports synthetic fuels are produced and which voyages are most suitable to using synthetic fuels.

2.4 Mixed-integer linear programming (MILP)

Let us first introduce the general linear program (LP).

Definition 1 *A linear program is of the form*

$$\begin{aligned} &\text{min. } cx \\ &\text{s.t. } Ax \leq b \\ &\quad x \geq 0, \end{aligned} \tag{1}$$

where A is a m by n matrix, b is a m-dimensional column vector, c is a n-dimensional row vector, and x is a n-dimensional column vector of decision variables [22].

The linear function cx is minimized, while being subjected to the constraint that Ax is less than b.

Definition 2 *A mixed-integer linear program (MILP) is a linear program with the additional constraint that some variables must be integers. A MILP has the general structure of*

$$\begin{aligned} &\text{min. } cx + hy \\ &\text{s.t. } Ax + Gy \leq b \\ &\quad x \geq 0 \\ &\quad y \in \mathbb{N}^p, \end{aligned} \tag{2}$$

where A is m by n, G is m by p, c is a n-dimensional row vector, h is a p-dimensional row vector, b is a m-dimensional column vector, x is a n-dimensional column vector of decision variables, and y is a p-dimensional column vector of integer decision variables [22].

Variations exists such as integer programs (IP) where all decision variables have to be integers, or binary integer program (BIP) where all decision variables are constrained to be binary. Even though, the structure of the MILP (2) is very similar to the LP (1), simply rounding the solution given by the LP relaxation, which is the LP you get by ignoring the integer constraint, is not at all sufficient to solve a MILP [22]. Consider the problem max. $x_1 + \frac{16}{25}x_2$, subject to the feasible set shown in Figure 3, where the blue dots are the feasible points bounded by the two blue lines [23]. Solving the LP relaxation gives the solution (376/193, 950/193), while the optimal integer solution is (5, 0). Not only does rounding the LP relaxation solution not give the optimal integer solution, it is not even feasible in this particular case.

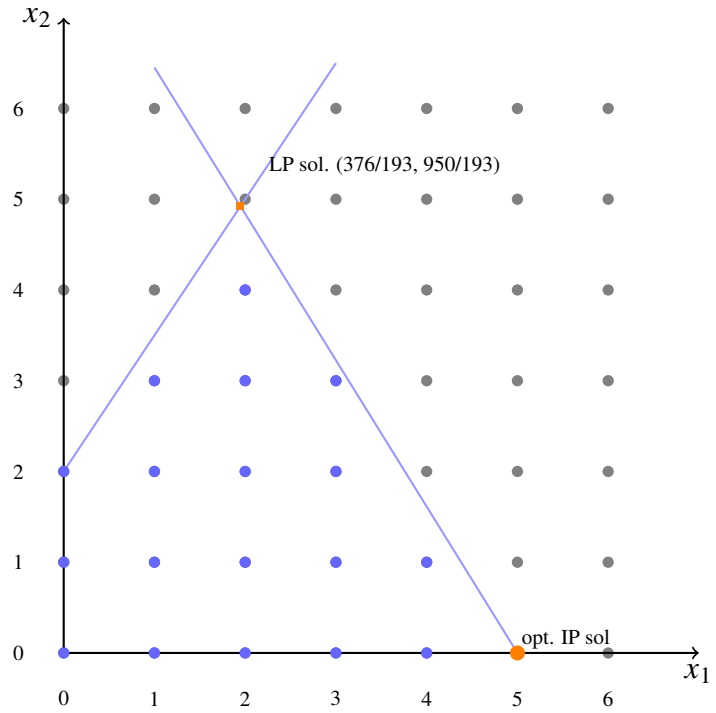

Figure 3: Graphical representation of the feasible region of the example [23].

Since rounding is not possible, enumeration could be another possibility, since the intersection of the problem constraints with the set of integers is usually finite. However, this is in practice only possible for very small problems with few decision variables.

To solve MILP problems, let us first introduce the notion of bounds [22]. Let $\mathbf{z}$ be the optimal objective value to Problem (2). If we can find a sequence of lower bounds

$$\underline{z}_1 < \underline{z}_2 < \ldots < \underline{z}_s \leq \mathbf{z}, \tag{3}$$

and a sequence of upper bounds

$$\bar{z}_1 > \bar{z}_2 > \ldots > \bar{z}_t \geq \mathbf{z}, \tag{4}$$

we can then get a suitable tight bound ($\bar{z} \geq \mathbf{z} \geq \underline{z}$) for the optimal objective value $\mathbf{z}$. In this context, we usually talk about two types of bounds, primal bounds and dual bounds. Primal bounds are found from a feasible solution to the problem (not necessarily optimal). For a minimization problem, primal bounds are upper bounds. Dual bounds are often found by an infeasible solution, i.e., a solution that is outside the feasible set. In the context of MILP, dual bounds can be found by solving the LP relaxation. For a minimization problem, dual bounds are lower bounds.

To solve a regular LP (1) the simplex method can be used [24]. We can note that due to the linearity of a LP, an optimal solution will always be at a vertex of the feasible region made up by the equality constraints. Thus, if we find a feasible vertex, we can move along the edge that improves the objective function the most, and repeat until it can no longer be improved. Then the optimal solution has been found.

However, this approach does not work for MILP (2), since the feasible region is not continuous, and the vertices made up by the equality constraints are usually not feasible, e.g. see Figure 3. However, we can solve the LP relaxation of the MILP problem, choose one of the decision variables x_i and branch the problem into two subproblems with additional constraints $x_i \leq \lfloor x_i^* \rfloor$ and $x_i \geq \lceil x_i^* \rceil$. We can then continue solving the subproblems in the same way by branching and adding constraints until an integer solution is found, however, the number of problems to solve then grows exponentially. But if lower or upper bounds can be found during the process, we can discard entire "branches" from the tree so that we only try to solve subproblems that can potentially improve our solution. This method is called branch and bound [22]. Since solving one MILP involves solving usually a large amount of LPs, potentially exponentially many, it is clear why solving MILPs is so computationally difficult.

2.5 Multiobjective optimization

Unlike the problem discussed in Section 2.4, let us now consider a problem with several objective functions. These problems are called multiobjective optimization problems. The structure of a multiobjective optimization problem is as follows,

$$\begin{aligned} &\text{min. } \{f_1(x), f_2(x), ..., f_k(x)\} \\ &\text{s.t. } x \in S. \end{aligned} \tag{5}$$

Here, $x = (x_1, x_2, ..., x_n)$ are the decision variables in the feasible set S, and we have $k \geq 2$ objective functions [25]. For example, S can be the feasible set of a LP (Definition 1) or a MILP (Definition 2).

Definition 3 *Let's denote the objective function vector by* $\boldsymbol{f(x)} = (f_1(x), f_2(x), ..., f_k(x))$, *where* $f_i(x) : \mathbb{R}^n \to \mathbb{R}, i \in \{1, ..., k\}$, *are the individual objective functions. The feasible objective region, is the image of the feasible set S, denoted by* $Z = \boldsymbol{f}(S) \subset \mathbb{R}^k$.

Unlike single-objective optimization problems, there is usually no single decision vector that minimizes all objective functions [25]. This is because the objective functions in multiobjective optimization problems are usually conflicting in some way. They may also be in different units which makes comparisons between two objective functions, and scalarisation difficult.

Since the number of decision variables n is much greater than the number of objective functions k, we usually study multiobjective optimization problems from the objective space [25]. Here a problem arises, there is no complete order for the objective space, e.g. while $(1, 1)$ is less than $(2, 2)$, $(1, 2)$ and $(2, 1)$ cannot be traditionally compared. However, we can study certain vectors from the feasible objective region Z, i.e., vectors such that improving one component cannot be done without deteriorating some other one. Such vectors are called Pareto optimal vectors.

Definition 4 *A vector* $x^* \in S$ *is Pareto optimal if there does not exist another decision vector* $x \in S$ *such that* $f_i(x) \leq f_i(x^*)$ *for all* $i = 1, ..., k$ *and* $f_j(x) < f_j(x^*)$ *for at least one index* j *[25]. The set of all Pareto optimal vectors is called the Pareto optimal set.*

Corollary 4.1 *An objective vector $f(x^*) \in Z$ is Pareto optimal if its corresponding vector $x \in S$ is Pareto optimal [25]. These are also sometimes called non-dominated vectors.*

Figure 4 shows the Pareto optimal set for a biobjective minimization problem in bold. The Pareto optimal set is not necessarily finite in size. There also exists a weaker

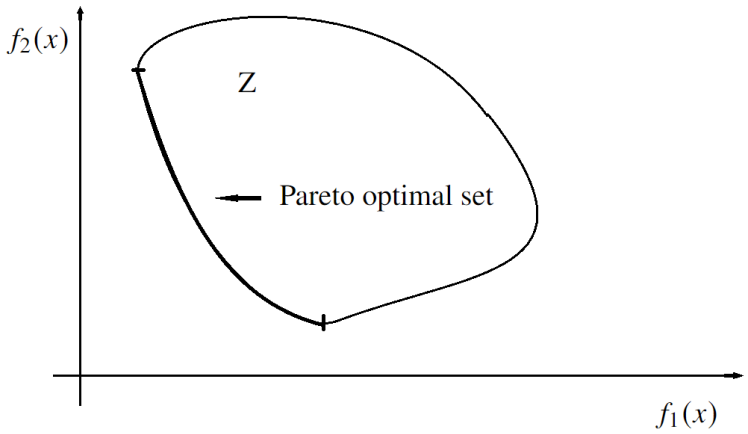

Figure 4: The Pareto optimal set is the bolded line [25].

version of Pareto optimality.

Definition 5 *A vector $x^* \in S$ is **weakly** Pareto optimal if there does not exist another vector $x \in S$ such that $f(x) < f_i(x^*)$ for all $i = 1, ..., k$ [25].*

Corollary 5.1 *An objective vector $f(x^*) \in Z$ is weakly Pareto optimal if its corresponding vector $x \in S$ is weakly Pareto optimal [25].*

While Pareto optimality 4 is preferred to weakly Pareto optimality 5, weak Pareto optimal points are usually easier to find and verify. There are several ways to generate, at least parts of, the Pareto optimal set [25]. These methods are also called posteriori methods, since no prior knowledge on how the different objectives are valued is assumed. Unfortunately however, such methods are usually computationally expensive. Some methods can only find Pareto optimal vectors that lie on the convex hull of the feasible objective region Z. This thesis will present four methods from literature, the weighting method, the ε-constraint method, the weighted Tchebycheff method, and the boxing method.

2.5.1 Weighting method

For the weighting method, the original problem (5) is transformed to a single objective problem by taking a weighted sum of the objective functions [25].

Definition 6 *The weighting problem, defined as*

$$\begin{aligned} \text{min.} \sum_{i=1}^{k} w_i f_i(x) \\ \text{s.t. } x \in S, \end{aligned} \tag{6}$$

where $w_i \geq 0$ *for all* $i = 1, ..., k$ *and* $\sum_{i=1}^{k} w_i = 1$.

The weighting problem has only one objective, the weighted sum, so it can be solved using traditional optimization methods. By varying the weights, different Pareto optimal points can be found. The weighting problem is very easy to implement, however, not all Pareto optimal points can be found unless the feasible objective region Z is convex. Solutions to the weighting method are guaranteed to be weakly Pareto optimal, and Pareto optimal if all weights w_i are positive.

2.5.2 ε-constraint method

For the ε-constraint method, one objective function is chosen to be minimized, while the rest of the objective functions are converted into constraints [25]. These constraints are made by setting an upper bound to the corresponding objective functions.

Definition 7 *The* ε*-constraint problem, defined as*

$$\begin{aligned} \text{min. } & f_j(x) \\ \text{s.t. } & f_i(x) \leq \varepsilon_i \; \forall i = 1, ..., k, \; i \neq j \\ & x \in S, \end{aligned} \tag{7}$$

where $j \in \{1, ..., k\}$, *and* ε_i *are the upper bounds.*

Again, the multiobjective problem has been turned into a single-objective problem, and different Pareto optimal solutions can be found by varying the upper bounds ε_i. It is theoretically possible to find all Pareto optimal solutions with the ε-constraint method. However, it is more computationally expensive due to extra constraints. The ε-constraint method can handle nonconvex problems. Solutions to the ε-constraint method are guaranteed to be weakly Pareto optimal.

2.5.3 Weighted Tchebycheff method

For the weighted Tchebycheff method, the concept of the ideal objective vector needs to be introduced [25].

Definition 8 *The ideal objective vector* $\mathbf{z}^* \in \mathbb{R}^k$ *is defined so that each component* z_i *is the minimum of* $f_i(x)$ *subject to* $x \in S$, *for each* $i = 1, ..., k$.

We can then minimize the weighted distance between the objective vector $\mathbf{f(x)}$ and the ideal vector $\mathbf{z}^*$. When using the max-norm, it is called the weighted Tchebycheff problem.

Definition 9 *The weighted Tchebycheff problem, defined as*

$$\begin{aligned} \text{min.} \max_{i=1,\dots k} \{w_i(f_i(x) - z_i)\} \\ \text{s.t. } x \in S, \end{aligned} \tag{8}$$

where $w_i \geq 0 \; \forall i = 1, \dots, k$ *and* $\sum_{i=1}^{k} w_i = 1$.

The problem in Definition 9 is not in the form of a MILP (Definition 2). It can be transformed into a MILP form, if S is corresponding to a MILP.

Corollary 9.1 *The MILP form of the weighted Tchebycheff problem is*

$$\begin{aligned} &\text{min. } \Delta \\ &\text{s.t. } \Delta \geq w_i(f_i(x) - z_i) \; \forall i = 1, \dots, k \\ &\quad x \in S, \end{aligned} \tag{9}$$

where $\Delta \in \mathbb{R}$ *is an additional decision variable.*

By varying the weights, different Pareto optimal solutions can be found. The weighted Tchebycheff Problem (8) is guaranteed to find at least one Pareto optimal solution. If several are found for one set of weights, the one which is Pareto optimal has to be verified. Like the ε-constraint method, the weighted Tchebycheff method can handle non-convex problems.

2.5.4 Boxing method

The three previous methods are very general in the sense that they produce solutions for all types of problems. However, since the model in this thesis possesses some special properties, we might want to exploit them. The boxing method introduced in [26] is aimed specifically for biobjective problems with discrete feasible objective regions. First some concepts need to be introduced.

Definition 10 *The biobjective lexicographic minimization problem is defined as*

$$\begin{aligned} \text{lex min. } (f_1(x), f_2(x)) \\ \text{s.t. } x \in S, \end{aligned} \tag{10}$$

where lex min. *denotes the lexicographic minimum [27]. The lexicographic minimum means that the first objective is more important than the second one, and will be minimized first. Only if the first minimization does not yield a unique solution will the second objective be minimized, with the condition that the first objective remains the same.*

We can illustrate this with an example. Figure 5 shows an example feasible objective region $\mathbf{Z}$. If we first minimize the second objective f_2, we get the lexicographic optimum a, since f_1 cannot then change without affecting f_2. However, if we instead first minimize the first objective f_1, we can then still minimize the second objective f_2 without affecting f_1. Thus, the other lexicographic optimum is b.

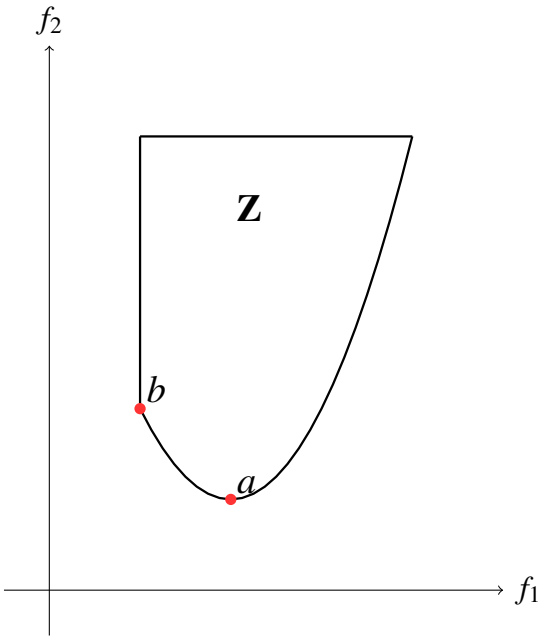

Figure 5: Example feasible objective region $\mathbf{Z}$, and the two lexicographic minima a and b.

With this information we can introduce the lexicographic ε-constraint method. Note that here we consider $f_2(x)$ to be more important.

Definition 11 *The lexicographic ε-constraint problem, defined as*

$$\begin{aligned} &\text{lex min. } (f_2(x), f_1(x)) \\ &\text{s.t. } f_1(x) \leq \varepsilon \\ &x \in S, \end{aligned} \tag{11}$$

where the objectives are lexicographically minimized with the additional constraint as in Definition 7 [26].

The idea behind the Boxing method is, given a box (rectangle) containing all Pareto optimal solutions, the box can be iteratively divided into two smaller boxes still containing all Pareto optimal solutions [26]. Stopping when a suitable number of Pareto optimal solutions have been found is guaranteed to yield a good representation of the complete Pareto optimal set.

Let $R(z^1, z^2)$ be the rectangle defined by z^1 as the upper left point and z^2 as the lower right point, and $a(R(z^1, z^2))$ be the area of said rectangle [26]. Below a slight

modification of the Boxing method is presented. Let the two initial points for the boxing algorithm be

$$z^1 = (z_1^1, z_2^1) = \operatorname*{lex\,min}_{x \in S} (f_1(x), f_2(x)) \text{ and}$$
$$z^2 = (z_1^2, z_2^2) = \operatorname*{lex\,min}_{x \in S} (f_2(x), f_1(x)).$$

The complete Pareto optimal set is a subset of $R(z^1, z^2)$. Let $\varepsilon = (z_1^1 + z_1^2)/2$. Then let x^* be optimal for problem (11), and z^* be $(f_1(x^*), f_2(x^*))$. z^* is then Pareto optimal. We then define a point $p = (\varepsilon, z_2^*)$. We can then notice that the rectangles $R_1 = R(z^1, z^*)$ and $R_2 = R(p, z^2)$ contain all Pareto optimal solutions, and combined are less than half the area of the original rectangle. We then chose the largest of the remaining rectangles and repeat the steps. When the remaining rectangles are sufficiently small we stop the algorithm.

2.5.5 Decision maker

A concept that might be needed for solving multiobjective optimization problems is a decision maker (DM) [25]. While every Pareto optimal solution is mathematically equally optimal, in the real world we might want to chose a single solution. This is where the decision maker is needed. The decision maker is a person or a group with more insight into the given problem, and is able to provide preference statements between the different objectives. E.g. in this context a decision maker might say that reducing emissions is more important than keeping costs down. Such statements can then be used to add additional constraints to reduce the size of the Pareto optimal set.

3 Research methods

This section the research methods used in this thesis. First, the optimization model is presented. Then a small example model is solved and presented. The implemented multiobjective solvers are then presented, along with a robust way of categorizing the ports based on the multiobjective solutions. Finally the data used for the model is presented. Figure 6 shows a flowchart of how the model is structured.

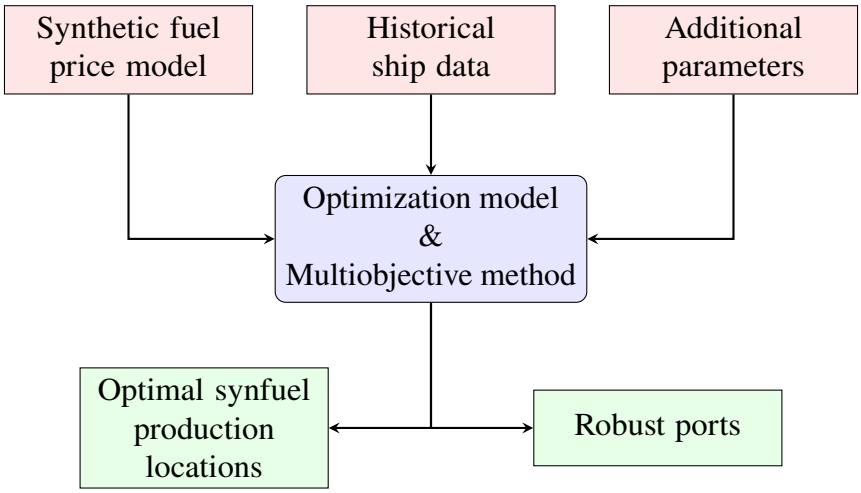

Figure 6: Flow chart showing how the complete model will work. Inputs into the model are shown in red, and outputs are shown in green.

3.1 Optimization model

The objective is to develop a model that finds optimal ports where decarbonised bunkering options could be placed. We want to maximize the reduction in CO_2 emissions, i.e., maximize the uptake of decarbonised synfuels. We also want to minimize the costs related to these new synfuels. These two objectives are conflicting, i.e., reducing emissions by a large amount is expensive.

The synfuels can be either produced locally at the ports where they are needed, or some can be bought from the global market and shipped to the chosen port. Producing fuels locally has a price dependent on location, while purchasing from the market has a set price, independent of location. If local production of a certain fuel is considered, more than a set minimum amount needs to be produced per year. Purchasing from the market is assumed to have infinite capacity. If purchasing from the market is done, a minimum amount is enforced. It is assumed that the cost of the bunkering itself is negligible. If a voyage is to be done using a synthetic fuel, the ship needs to bunker at the port of origin.

The model parameters are the inputs in red in Figure 6, and the decision variables are the outputs we get, in green. First the nomenclature for the model is presented. Then the model itself is presented.

Sets

$i, j \in P$	Set of ports
$k \in K$	Set of synfuels
$k \in H \subset K$	Subset of synfuels that are hydrogen
$k \in A \subset K$	Subset of synfuels that are ammonia
$t \in T$	Set of ship types

Decision variables

$x_{ijkt} \in \mathbb{N}$	Amount of voyages from port i to j for ship type t, assigned with fuel k.
$b_{ik} \geq 0$	Amount of local production for fuel type k in harbour i (MWh/year).
$m_{ik} \geq 0$	Amount of fuel k bought from the market to harbour i (MWh/year).
$y^p_{ik} \in \{0, 1\}$	Binary indicator variable if fuel k is produced in port i.

Parameters

V_{ijt}	Number of voyages from from port i to j for ship type t.
E_{ijt}	Average energy needed per voyage from port i to j for ship type t (MWh).
p^1_{ik}	Cost of fuel k produced locally in harbour i (€/MWh).
p^2_k	Market price for fuel k (€/MWh).
β^p_k	Minimum allowable production rate for fuel k (MWh/year).
α	Emission constant (g_{CO2eq}/MWh).
z	Maximum energy that can be served by hydrogen per voyage (MWh).
μ	Efficiency factor.

Constraints

Constraint (12) makes sure that we do not assign more fuels than there are voyages per route. E.g. if there are 10 recorded voyages from port A to port B, we can switch at most 10 routes to new synfuels.

$$\sum_{k \in K} x_{ijkt} \leq V_{ijt}, \ \forall i, j \in P, \forall t \in T \tag{12}$$

Constraint (13) makes sure we assign as much synthetic fuel, to voyages that leave from port i, as what is produced in, and what is bought to port i, for every fuel k that can be bought from the market. E.g. if 500 MWh of ammonia is produced in, and 500 MWh is bought to port A, exactly 1000 MWh of ammonia is assigned to voyages that leave from port A. The efficiency factor μ is used to quantify that fuel cells are more efficient than ICE. Since the energy needed E_{ijt} is for an ICE burning traditional fuels, we multiply by the efficiency factor μ to get the energy needed for a fuel cell ship.

$$\sum_{j \in P} \sum_{t \in T} x_{ijkt} \cdot E_{ijt} \cdot \mu = b_{ik} + m_{ik}, \ \forall i \in P, \forall k \in A \tag{13}$$

Constraint (14) makes sure that we assign as much synthetic fuel, to voyages that leave from port i, as what is produced in port i, for every fuel k that cannot be bought from the market.

$$\sum_{j \in P} \sum_{t \in T} x_{ijkt} \cdot E_{ijt} \cdot \mu = b_{ik}, \ \forall i \in P, \forall k \in H \tag{14}$$

Constraint (15) states that only voyages that on average have an energy requirement of less than z can use hydrogen. This constraint tries to capture that only relatively short voyages with a relatively small energy need can use hydrogen, due to its lesser volumetric density.

$$x_{ijkt} \cdot E_{ijt} \cdot \mu \leq z, \ \forall i, j \in P, \forall k \in H, \forall t \in T \tag{15}$$

We want to impose a constraint that makes sure that if we decide to produce a synthetic fuel it has to be above a certain minimum rate. For ammonia, there is a strict minimum amount. However, since producing ammonia already requires hydrogen, producing hydrogen only requires that ammonia and hydrogen production is above the set minimum. Constraint (16) makes sure that if ammonia is produced, it is produced above a certain minimum amount, in every port. Constraint (17) makes sure that if hydrogen is produced, the sum of hydrogen and ammonia production is above a certain minimum, in every port.

$$b_{ik} \geq \beta_k^p \cdot y_{ik}^p, \ \forall i \in P, \forall k \in A \tag{16}$$

$$\sum_{k' \in K} b_{ik'} \geq \beta_k^p \cdot y_{ik}^p, \ \forall i \in P, \forall k \in H \tag{17}$$

Constraint (18) is a big M constraints to allow for no production, where M is a sufficiently big constant.

$$b_{ik} \leq M \cdot y_{ik}^p, \ \forall i \in P, \forall k \in K \tag{18}$$

However, constraint (18) is a weak formulation, since it is difficult to determine a single M that is large enough to not make any solution infeasible, but also small enough to make potential LP relaxations partly integer solutions. Thus the constraints can be reformulated so that for every i, we assign a different upper bound N_i. This N_i is the total amount of energy needed to satisfy all voyages leaving port i, and is determined from the available data. Constraint (19) is a stronger formulation of constraint (18), and will be used instead.

$$b_{ik} \leq N_i \cdot y_{ik}^p, \ \forall i \in P, \forall k \in K \tag{19}$$

Objective functions

Objective function (20) captures the emissions that are reduced by switching to synfuels. α represents tons of CO_2 equivalent emissions per MWh of HFO burned. This objective function (20) is maximized, so to turn it into a minimization problem, $-f_1$ is minimized.

$$f_1 = \sum_{i \in P} \sum_{j \in P} \sum_{k \in K} \sum_{t \in T} x_{ijkt} \cdot E_{ijt} \cdot \alpha \tag{20}$$

Objective function (21) represents the total yearly cost in €/year. The yearly cost is comprised of the synfuels that are locally produced as well as the synfuels that are bought from the market. This objective function (21) is minimized.

$$f_2 = \sum_{i \in P} \sum_{k \in K} b_{ik} \cdot p^1_{ik} + \sum_{i \in P} \sum_{k \in A} m_{ik} \cdot p^2_k \tag{21}$$

The full model then becomes

$$\begin{aligned}
\text{min. } & \{-(\sum_{i \in P} \sum_{j \in P} \sum_{k \in K} \sum_{t \in T} x_{ijkt} \cdot E_{ijt} \cdot \alpha), \ \sum_{i \in P} \sum_{k \in K} b_{ik} \cdot p^1_{ik} + \sum_{i \in P} \sum_{k \in K} m_{ik} \cdot p^2_k\} \\
\text{s.t. } & \sum_{k \in K} x_{ijkt} \leq V_{ijt}, \ \forall i, j \in P, \forall t \in T \\
& \sum_{j \in P} \sum_{t \in T} x_{ijkt} \cdot E_{ijt} \cdot \mu = b_{ik} + m_{ik}, \ \forall i \in P, \forall k \in A \\
& \sum_{j \in P} \sum_{t \in T} x_{ijkt} \cdot E_{ijt} \cdot \mu = b_{ik}, \ \forall i \in P, \forall k \in H \\
& x_{ijkt} \cdot E_{ijt} \cdot \mu \leq z, \ \forall i, j \in P, \forall k \in H, \forall t \in T \\
& b_{ik} \geq \beta^p_k \cdot y^p_{ik}, \ \forall i \in P, \forall k \in A \\
& \sum_{k' \in K} b_{ik'} \geq \beta^p_k \cdot y^p_{ik}, \ \forall i \in P, \forall k \in H \\
& b_{ik} \leq N_i \cdot y^p_{ik}, \ \forall i \in P, \forall k \in K \\
& x_{ijkt} \in \mathbb{N}, \ \forall i, j \in P, \forall k \in K, \forall t \in T \\
& b_{ik} \geq 0, \ \forall i \in P, \forall k \in K \\
& m_{ik} \geq 0, \ \forall i \in P, \forall k \in K \\
& y^p_{ik} \in \{0, 1\}, \ \forall i \in P, \forall k \in K.
\end{aligned} \tag{22}$$

3.2 Example model solution

To illustrate this model and give a small example, let us consider a small, scaled down version. Let us consider only two ports a and b, only one synthetic fuel, and only one ship type. This fuel costs 110 €/MWh in port a and 160 €/MWh in port b. Fuel cannot be bought from the market. There are 3 voyages from a to b, and 5 voyages from b to a, within a certain time frame, that all require 500 MWh worth of fuel. If we install local production of the synthetic fuel, a minimum of 1000 MWh needs to be produced within the same time frame. Let the emission constant be 0.3 t_{CO2e}/MWh. This simple model is solved by enumerating all feasible solutions and eliminating solutions that are not Pareto optimal. Figure 7 shows the complete Pareto set.

Table 1 shows the Pareto optimal solutions to the example problem, where x_{ab} and x_{ba} is the number of voyages were we use the synthetic fuel from a to b, and b to a respectively. Variables b_a and b_b is the produced amount of synthetic fuel in port a and b respectively. Some noteworthy properties of the Pareto optimal set shown in Figure 7 for this model can be observed. The Pareto optimal set does not lie entirely

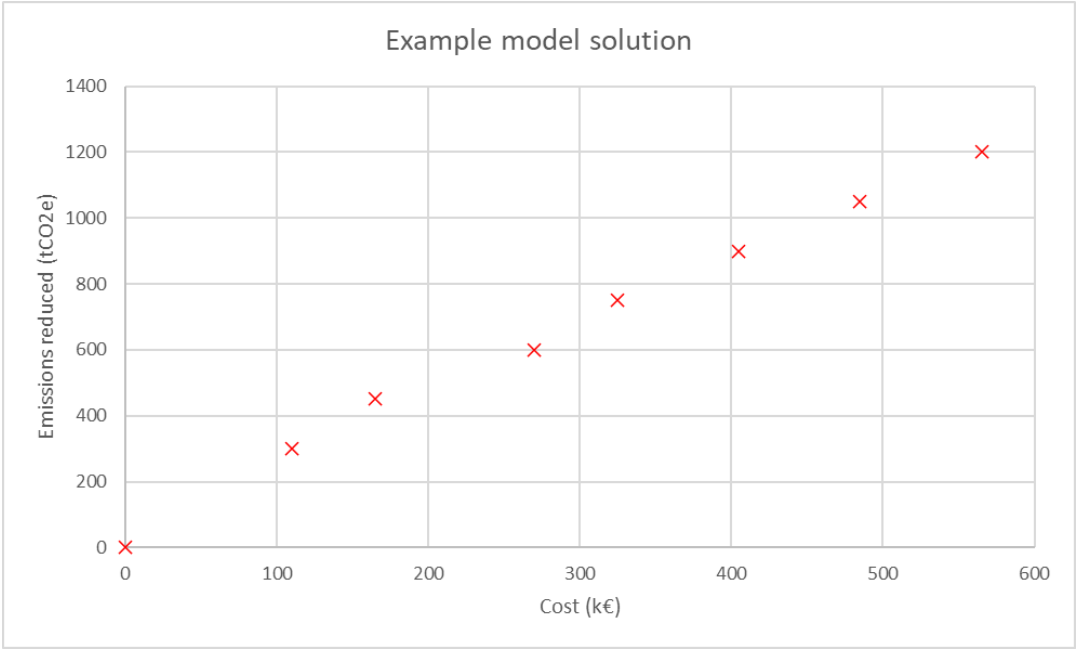

Figure 7: Pareto optimal set for the example model.

on the convex hull of the feasible objective region. Thus, the weighting method (6) might not be able to find all Pareto optimal solutions. The Pareto optimal set is also not continuous, but consists of discrete points.

x_{ab}	x_{ba}	b_a	b_b	Objective 1 (t_{CO2e})	Objective 2 (k€)
0	0	0	0	0	0
2	0	1000	0	300	110
3	0	1500	0	450	165
2	2	1000	1000	600	270
3	2	1500	1000	750	325
3	3	1500	1500	900	405
3	4	1500	2000	1050	485
3	5	1500	2500	1200	565

Table 1: Solutions to the example model, every row is a Pareto optimal solution.

3.3 Multiobjective methods

The four methods introduced in section 2.5 are implemented. First is the weighting method in Definition 6. The method then becomes

$$
\begin{aligned}
\text{min. } & w_1(-\sum_{i\in P}\sum_{j\in P}\sum_{k\in K}\sum_{t\in T} x_{ijkt}\cdot E_{ijt}\cdot\alpha) + \ w_2(\sum_{i\in P}\sum_{k\in K} b_{ik}\cdot p^1_{ik} + \sum_{i\in P}\sum_{k\in K} m_{ik}\cdot p^2_k) \\
\text{s.t. } & \sum_{k\in K} x_{ijkt} \le V_{ijt},\ \forall i,j\in P, \forall t\in T \\
& \sum_{j\in P}\sum_{t\in T} x_{ijkt}\cdot E_{ijt}\cdot\mu = b_{ik} + m_{ik},\ \forall i\in P, \forall k\in A \\
& \sum_{j\in P}\sum_{t\in T} x_{ijkt}\cdot E_{ijt}\cdot\mu = b_{ik},\ \forall i\in P, \forall k\in H \\
& x_{ijkt}\cdot E_{ijt}\cdot\mu \le z,\ \forall i,j\in P, \forall k\in H, \forall t\in T \\
& b_{ik} \ge \beta^p_k\cdot y^p_{ik},\ \forall i\in P, \forall k\in A \\
& \sum_{k'\in K} b_{ik'} \ge \beta^p_k\cdot y^p_{ik},\ \forall i\in P, \forall k\in H \\
& b_{ik} \le N_i\cdot y^p_{ik},\ \forall i\in P, \forall k\in K \\
& x_{ijkt}\in\mathbb{N},\ \forall i,j\in P, \forall k\in K, \forall t\in T \\
& b_{ik}\ge 0,\ \forall i\in P, \forall k\in K \\
& m_{ik}\ge 0,\ \forall i\in P, \forall k\in K \\
& y^p_{ik}\in\{0,1\},\ \forall i\in P, \forall k\in K
\end{aligned}
\tag{23}
$$

where $w_1, w_2 \ge 0$ and $w_1 + w_2 = 1$. The coefficients w_1 and w_2 are evenly distributed between 0 and 1, satisfying the constraint.

Second is the ε-constraint method in Definition 7. The ε-constraint problem looks

as follows

$$
\begin{aligned}
\text{min.}\ & \sum_{i\in P}\sum_{k\in K} b_{ik}\cdot p^1_{ik} + \sum_{i\in P}\sum_{k\in K} m_{ik}\cdot p^2_k \\
\text{s.t.}\ & -\Big(\sum_{i\in P}\sum_{j\in P}\sum_{k\in K}\sum_{t\in T} x_{ijkt}\cdot E_{ijt}\cdot\alpha\Big) \le \varepsilon \\
& \sum_{k\in K} x_{ijkt} \le V_{ijt},\ \forall i,j\in P, \forall t\in T \\
& \sum_{j\in P}\sum_{t\in T} x_{ijkt}\cdot E_{ijt}\cdot\mu = b_{ik} + m_{ik},\ \forall i\in P, \forall k\in A \\
& \sum_{j\in P}\sum_{t\in T} x_{ijkt}\cdot E_{ijt}\cdot\mu = b_{ik},\ \forall i\in P, \forall k\in H \\
& x_{ijkt}\cdot E_{ijt}\cdot\mu \le z,\ \forall i,j\in P, \forall k\in H, \forall t\in T \\
& b_{ik} \ge \beta^p_k\cdot y^p_{ik},\ \forall i\in P, \forall k\in A \\
& \sum_{k'\in K} b_{ik'} \ge \beta^p_k\cdot y^p_{ik},\ \forall i\in P, \forall k\in H \\
& b_{ik} \le N_i\cdot y^p_{ik},\ \forall i\in P, \forall k\in K \\
& x_{ijkt}\in\mathbb{N},\ \forall i,j\in P, \forall k\in K, \forall t\in T \\
& b_{ik}\ge 0,\ \forall i\in P, \forall k\in K \\
& m_{ik}\ge 0,\ \forall i\in P, \forall k\in K \\
& y^p_{ik}\in\{0,1\},\ \forall i\in P, \forall k\in K
\end{aligned}
\tag{24}
$$

where ε is the upper bound for objective function f_1 (20). To find suitable values for ε we first note that the maximum that $-f_1$ can achieve is trivially when all x_{ijkt} are zero. This corresponds with no synfuels being assigned to any routes and thus no CO_2

reduced. To find the minimum of $-f_1$ we solve the following problem,

$$
\begin{aligned}
\text{min. } & -\Big(\sum_{i\in P}\sum_{j\in P}\sum_{k\in K}\sum_{t\in T} x_{ijkt}\cdot E_{ijt}\cdot\alpha\Big) \\
\text{s.t. } & \sum_{k\in K} x_{ijkt} \le V_{ijt},\ \forall i,j\in P, \forall t\in T \\
& \sum_{j\in P}\sum_{t\in T} x_{ijkt}\cdot E_{ijt}\cdot\mu = b_{ik}+m_{ik},\ \forall i\in P, \forall k\in A \\
& \sum_{j\in P}\sum_{t\in T} x_{ijkt}\cdot E_{ijt}\cdot\mu = b_{ik},\ \forall i\in P, \forall k\in H \\
& x_{ijkt}\cdot E_{ijt}\cdot\mu \le z,\ \forall i,j\in P, \forall k\in H, \forall t\in T \\
& b_{ik} \ge \beta_k^p\cdot y_{ik}^p,\ \forall i\in P, \forall k\in A \\
& \sum_{k'\in K} b_{ik'} \ge \beta_k^p\cdot y_{ik}^p,\ \forall i\in P, \forall k\in H \\
& b_{ik} \le N_i\cdot y_{ik}^p,\ \forall i\in P, \forall k\in K \\
& x_{ijkt}\in\mathbb{N},\ \forall i,j\in P, \forall k\in K, \forall t\in T \\
& b_{ik}\ge 0,\ \forall i\in P, \forall k\in K \\
& m_{ik}\ge 0,\ \forall i\in P, \forall k\in K \\
& y_{ik}^p\in\{0,1\},\ \forall i\in P, \forall k\in K
\end{aligned}
\tag{25}
$$

which tells us how much CO_2 emissions can be reduced if we ignore the costs. Thus, we optimize without the second objective. When the upper and lower bounds are known, ε can be evenly distributed between these bounds to find an even distribution of Pareto optimal solutions. The amount of Pareto optimal solutions can then be determined beforehand to a suitable number.

Then, the MILP form of the weighted Tchebycheff problem in Definition 9.1 can

be constructed. The model becomes as follows,

$$
\begin{aligned}
&\text{min. } \Delta \\
&\text{s.t. } \Delta \geq w_1(-\sum_{i\in P}\sum_{j\in P}\sum_{k\in K}\sum_{t\in T} x_{ijkt}\cdot E_{ijt}\cdot\alpha - \mathbf{z}_1) \\
&\quad \Delta \geq w_2(\sum_{i\in P}\sum_{k\in K} b_{ik}\cdot p^1_{ik} + \sum_{i\in P}\sum_{k\in K} m_{ik}\cdot p^2_k - \mathbf{z}_2) \\
&\quad \sum_{k\in K} x_{ijkt} \leq V_{ijt},\ \forall i,j \in P, \forall t \in T \\
&\quad \sum_{j\in P}\sum_{t\in T} x_{ijkt}\cdot E_{ijt}\cdot\mu = b_{ik} + m_{ik},\ \forall i \in P, \forall k \in A \\
&\quad \sum_{j\in P}\sum_{t\in T} x_{ijkt}\cdot E_{ijt}\cdot\mu = b_{ik},\ \forall i \in P, \forall k \in H \\
&\quad x_{ijkt}\cdot E_{ijt}\cdot\mu \leq z,\ \forall i,j \in P, \forall k \in H, \forall t \in T \\
&\quad b_{ik} \geq \beta^p_k \cdot y^p_{ik},\ \forall i \in P, \forall k \in A \\
&\quad \sum_{k'\in K} b_{ik'} \geq \beta^p_k \cdot y^p_{ik},\ \forall i \in P, \forall k \in H \\
&\quad b_{ik} \leq N_i \cdot y^p_{ik},\ \forall i \in P, \forall k \in K \\
&\quad x_{ijkt} \in \mathbb{N},\ \forall i,j \in P, \forall k \in K, \forall t \in T \\
&\quad b_{ik} \geq 0,\ \forall i \in P, \forall k \in K \\
&\quad m_{ik} \geq 0,\ \forall i \in P, \forall k \in K \\
&\quad y^p_{ik} \in \{0,1\},\ \forall i \in P, \forall k \in K
\end{aligned}
\tag{26}
$$

where $w_1, w_2 \geq 0$, $w_1 + w_2 = 1$ and $\mathbf{z}_1, \mathbf{z}_2$ are the ideal objective vectors. $\mathbf{z}_2$ is trivially zero and can be omitted. $\mathbf{z}_1$ is the solution to Problem (25). The coefficients w_1 and w_2 are evenly distributed between 0 and 1, satisfying the constraint.

Finally, for the Boxing method, the lexicographic ε- constraint method looks as

follows,

$$
\begin{aligned}
\text{lex min. } & \Big(\sum_{i\in P}\sum_{k\in K} b_{ik}\cdot p^1_{ik} + \sum_{i\in P}\sum_{k\in K} m_{ik}\cdot p^2_k, -\Big(\sum_{i\in P}\sum_{j\in P}\sum_{k\in K}\sum_{t\in T} x_{ijkt}\cdot E_{ijt}\cdot\alpha\Big)\Big) \\
\text{s.t. } & -\Big(\sum_{i\in P}\sum_{j\in P}\sum_{k\in K}\sum_{t\in T} x_{ijkt}\cdot E_{ijt}\cdot\alpha\Big) \le \varepsilon \\
& \sum_{k\in K} x_{ijkt} \le V_{ijt},\ \forall i,j\in P, \forall t\in T \\
& \sum_{j\in P}\sum_{t\in T} x_{ijkt}\cdot E_{ijt}\cdot\mu = b_{ik} + m_{ik},\ \forall i\in P, \forall k\in A \\
& \sum_{j\in P}\sum_{t\in T} x_{ijkt}\cdot E_{ijt}\cdot\mu = b_{ik},\ \forall i\in P, \forall k\in H \\
& x_{ijkt}\cdot E_{ijt}\cdot\mu \le z,\ \forall i,j\in P, \forall k\in H, \forall t\in T \\
& b_{ik} \ge \beta^p_k\cdot y^p_{ik},\ \forall i\in P, \forall k\in A \\
& \sum_{k'\in K} b_{ik'} \ge \beta^p_k\cdot y^p_{ik},\ \forall i\in P, \forall k\in H \\
& b_{ik} \le N_i\cdot y^p_{ik},\ \forall i\in P, \forall k\in K \\
& x_{ijkt}\in\mathbb{N},\ \forall i,j\in P, \forall k\in K, \forall t\in T \\
& b_{ik}\ge 0,\ \forall i\in P, \forall k\in K \\
& m_{ik}\ge 0,\ \forall i\in P, \forall k\in K \\
& y^p_{ik}\in\{0,1\},\ \forall i\in P, \forall k\in K
\end{aligned}
\tag{27}
$$

where ε will be iteratively updated like in Section 2.5.4.

3.4 Robust ports and Core index

While the Pareto optimal sets that are generated by the methods in Section 3.3 are great tools for a potential decision maker, the information they contain can be condensed even further. Here, the concept of robust choices will be introduced and then implemented, based on [28]. Let S^{Pareto} be the set of Pareto optimal vectors, excluding the trivial vectors which lead to both objectives being zero, and $s\in S^{Pareto}$ be the the individual Pareto optimal vectors. The trivial vectors, which mean nothing is produced, of course at no cost, are removed, since for analysis they are not a desirable solution. Let us then consider the variable $(y^p_{ik})_s$ which denotes if fuel k is produced in port i in the solution s.

Definition 12 *The ideal core index for port i and fuel k is*

$$
\mathrm{CI}^*(i,k) = \frac{|\{(y^p_{ik})_s | (y^p_{ik})_s = 1\}|}{|S^{Pareto}|}. \tag{28}
$$

The ideal core index for a given port and fuel is between 0 and 1. An ideal core index of one indicates that independently of preferences between reducing emissions

and keeping costs down, it is optimal to produce fuel k in port i. An ideal core index of zero means that it is never optimal to produce fuel k in port i. An ideal core index somewhere in between means that this particular fuel and port combination is included in some, but not all Pareto optimal solutions.

Definition 13 *We define three distinct sets of*

- *Core ports:* $\mathrm{CI}^*(i,k) = 1$
- *Borderline ports:* $0 < \mathrm{CI}^*(i,k) < 1$
- *Exterior ports:* $\mathrm{CI}^*(i,k) = 0$.

Here, the sets are defined separately for each fuel, since ammonia and hydrogen behave quite differently in the context of this model. From the perspective of the DM, it is clear that choosing to produce fuels in ports with an ideal core index of 1 is preferred while choosing to produce fuel in ports with an ideal core index of 0 should be avoided. Core ports can be considered robust, since they are always included in Pareto optimal solutions, regardless of the preference between the objectives.

Since the complete Pareto optimal set is not always able to be computed, let us introduce a slight modification to the ideal core index, called the core index.

Definition 14 *The core index for port i and fuel k is*

$$\mathrm{CI}(i,k) = \frac{|\{(y^p_{ik})_f | (y^p_{ik})_f = 1\}|}{|F|}, \tag{29}$$

where F is the computed subset of the Pareto optimal set, in the image space, and $f \in F$.

Most things that hold for the ideal core index also hold for the core index, i.e., a core index of one indicates that independently of preferences between reducing emissions and keeping costs down, it is optimal to produce fuel k in port i. However, some things becomes more difficult if we do not have the complete Pareto optimal set, which is usually the case when working with real world problems where computing the complete Pareto optimal set is infeasible. Instead, we rely on methods, such as those in Section 2.5 to compute a subset of the complete Pareto optimal set. The objective functions are not necessarily injective, such is the case in this thesis, which means that we might have several solutions for a single objective value. Which solution the solver actually computes is not completely random, it can e.g. be influenced by which variable the branching is done on during the branch and bound method, which is something that can be decided by the user in the Gurobi solver [29]. This means that if there are several solutions that have equal objective values, the solver has a preference, which is not necessarily known to the user. This means that there might be perfectly optimal solutions that might not appear as solutions, since the solver might not chose them, which especially means that using a low core index to decide against a certain port might be unjustified. To recommend against a port with core indices of zero, the root cause why the core indices are zero have to be identified first. For

example, if producing in that port is always infeasible, we can recommend against that port. However, a high core index still means that a particular port is present in many Pareto optimal solutions.

3.5 Data

3.5.1 Historical ship data

Historical ship data from the year 2023 is used. The data originated as AIS messages from ships, and is cleaned and prepared at VTT into a more manageable form.

Each data point in the dataset used for this thesis consisted of a single route for a single ship from one port to another, with ship length and width, as well as estimated power needed for that trip. A total of 173 ports of origin, and around 5000 routes were included. The first step in using this data is to cluster the ports into reasonable sized clusters for two reasons. The first reason is to make it easier to run the MILP model, since the amount of the integer variable x_{ijkt} grows by the number of ports to the power of two. Secondly we assume a local hydrogen or ammonia plant can serve several ports if they are close enough.

The ports were clustered using the K-means method [30]. The number of clusters is chosen to be 40. Table 2 shows the cluster id and the approximate place name for each cluster. Figure 8 shows the ports and their clusters, each cluster has its own color and the center of each cluster is marked with its id.

Cluster id	Place name	Cluster id	Place name
0	Hamburg	20	Oulu
1	Helsinki	21	St Petersburg
2	Norrköping	22	Thisted
3	Gdansk	23	Riga
4	Copenhagen	24	Södertälje
5	Kokkola	25	Klaipėda
6	Vyborg	26	Szczecin
7	Åland islands	27	Flensburg
8	Bornholm	28	Gotland
9	Aarhus	29	Åhus
10	Saremaa	30	Kotka
11	East Frisian peninsula	31	Tallinn
12	Kaliningrad	32	Sillamäe
13	Porvoo	33	Kiel
14	Gothenburg	34	Oskarshamn
15	Turku	35	Marstrand
16	Northern Sweden	36	Sassnitz
17	Ludza	37	Bremen
18	Gävle	38	Ekenäs
19	Rostock	39	Karlskrona

Table 2: Table with cluster ids and approximate place name.

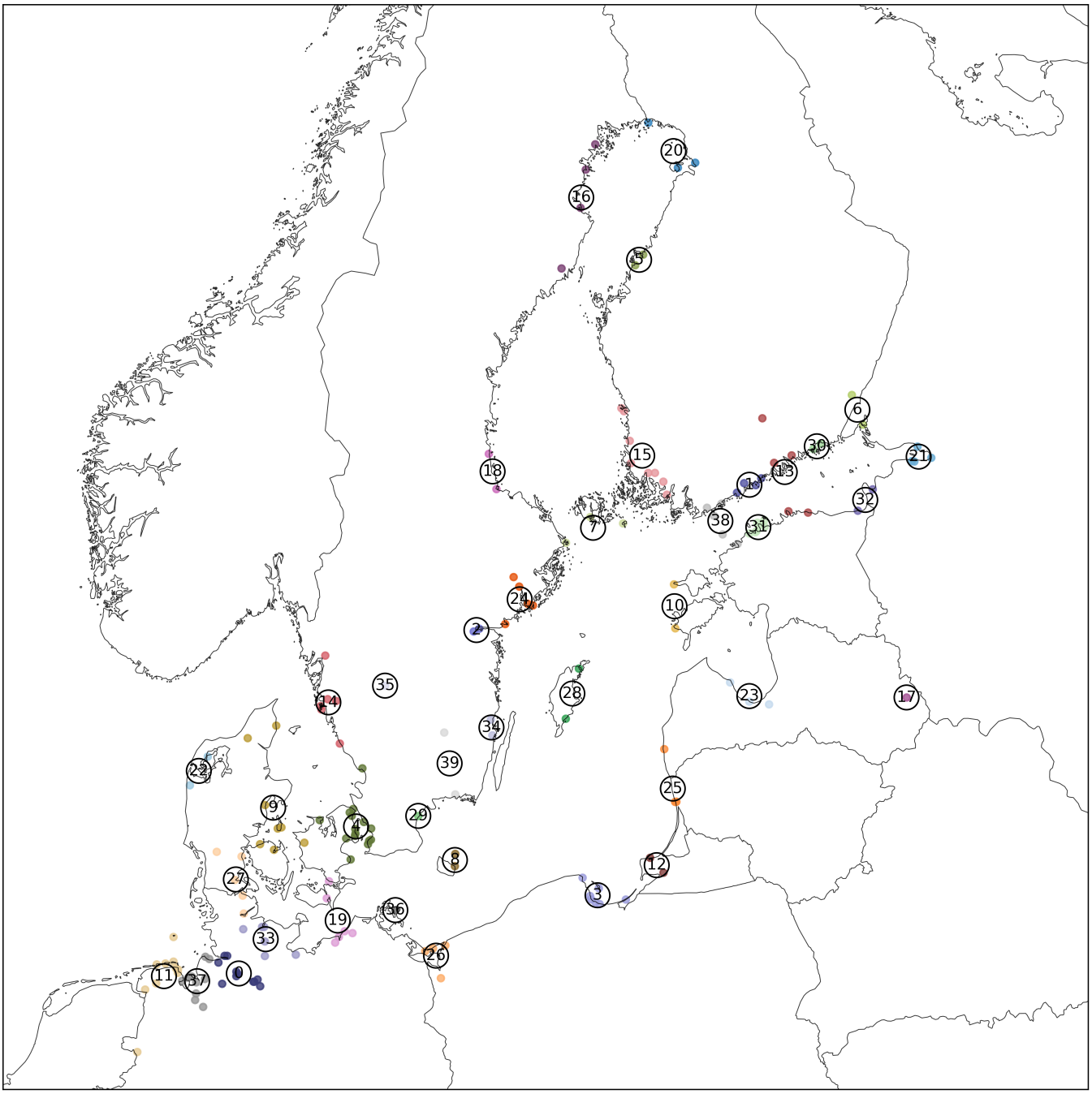

Figure 8: The Baltic sea ports and their respective clusters.

Since the data contains information about ship type and the size of the ship, we want to differentiate between size and type combinations to get more granular voyage data. The ship types included are **Bulk carrier**, and **Container ship**. The lengths of the ships are distributed between 115 m and 400 m. Figure 9 shows a histogram of the ship lengths. Note that one ship might appear several times in the data.

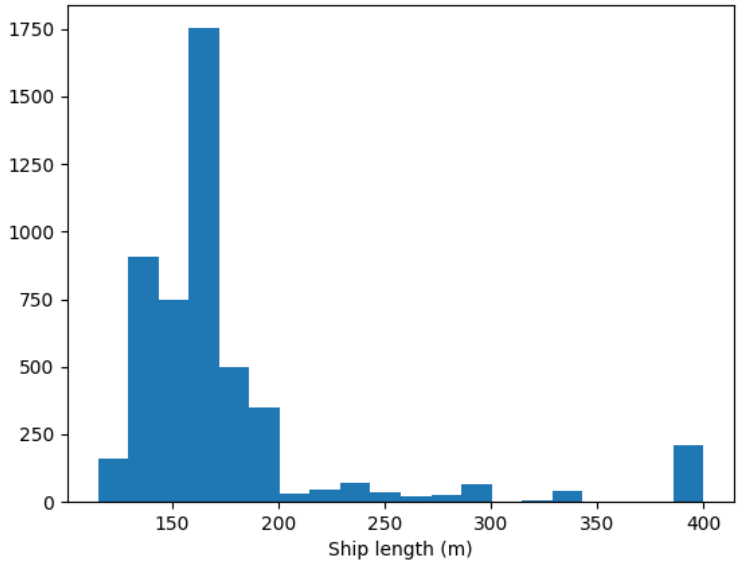

Figure 9: Histogram of the length of the ships in the routes.

We divide the ship lengths into three categories, shorter than 150 m, between 150 m and 250 m, and longer than 250 m. The ships are then be divided into six distinct groups, which are shown in Table 3. We then define a voyage such that it starts and

Ship group	Type	Length
1	Bulk carrier	< 150 m
2	Bulk carrier	≥ 150 m & < 250 m
3	Bulk carrier	≥ 250 m
4	Container ship	< 150 m
5	Container ship	≥ 150 m & < 250 m
6	Container ship	≥ 250 m

Table 3: Table showing how the different ships are grouped.

ends in a port cluster, for a single ship group. Thus, for every ship group all routes that start in the same port cluster and end in the same port cluster are aggregated such that the power needed is averaged. The headers for the final data, used for the model, are

- Origin
- Destination
- Ship group
- Average power needed
- Number of trips.

Note that voyages that start and end in the same port cluster are allowed, and are present in the data.

3.5.2 Price for hydrogen and ammonia

Figure 11 shows a breakdown of the estimated costs for a hydrogen valley in the northern Ostrobothina region in Finland [31]. This price model is used as a base. We clearly see that the electrolyzer and wind power purchase agreement (PPA) are the two largest parts of the total price. We assume that the cost of the electrolyzer

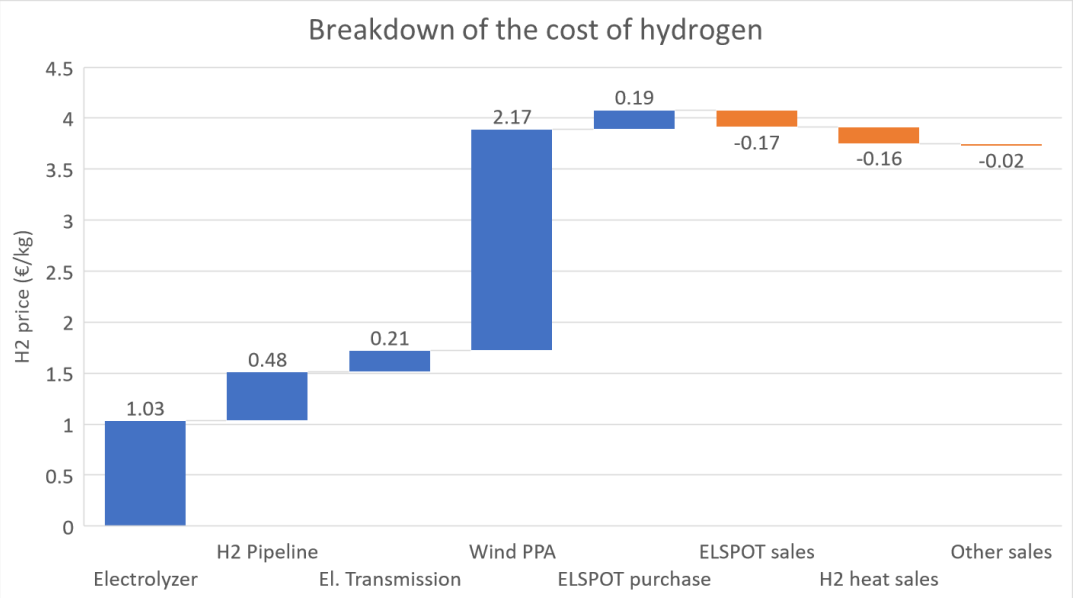

Figure 10: Breakdown of the cost of hydrogen for a hydrogen valley in northern Finland [31].

is the same everywhere around the Baltic sea. We also assume that all other parts (excluding electrolyzer and wind PPA costs) are the same in all countries. We can then use wind PPA cost data from different countries to estimate the cost of hydrogen from a hydrogen valley somewhere else in Europe. We notice that the Baltic countries and

Country	Wind PPA (€/MWh)
Sweden	34.5
Finland	35
Denmark	40
Poland	55
Germany	56

Table 4: Wind PPA data from several EU countries for the year 2022 from Bloomberg [32].

Russia is missing from this wind PPA price data. The levelised cost of wind electricity

has been estimated to be 80.07 €/MWh in Russia [33]. The levelised cost of wind electricity can be seen as a lower bound for a potential wind PPA price. Thus, we assume that the wind PPA price in Russia is 80 €/MWh. Due to the unavailability of data for the Baltic countries, we assume that their wind PPA price will be the average of Russia and Poland, which are their neighbours. This yields a price of 67.5 €/MWh. A more detailed breakdown for the cost of hydrogen in each country is available in Appendix A in Table A1.

Using the values from Table 4 [32] as well as the values for the Baltic countries and Russia, the wind PPA part from the cost breakdown in Figure 11 can be scaled for the different countries. Using the lower heating value of 33.33 kWh/kg, we can also get the cost per unit of energy [34]. Table 5 and Figure 11 shows the cost of hydrogen in 10 countries around the Baltic sea.

Country	**€/kg$_{H2}$**	**€/MWh$_{H2}$**
Sweden	3.70	111.0
Finland	3.73	111.9
Denmark	4.04	121.2
Poland	4.97	149.1
Germany	5.03	151.0
Baltic countries	5.75	172.4
Russia	6.52	195.6

Table 5: Prices for hydrogen in the countries surrounding the Baltic sea per kilogram and per MWh.

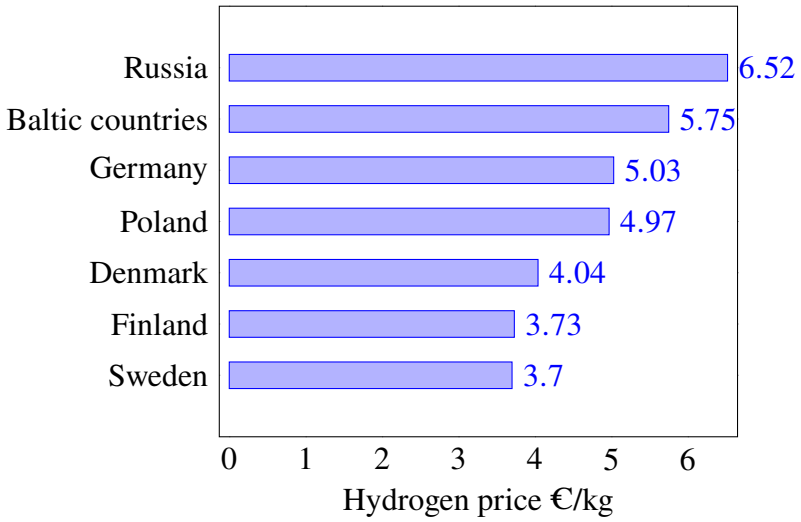

Figure 11: Bar chart with the cost of hydrogen in €/kg.

In this model, green ammonia is produced via Fischer-Trops synthesis. To estimate the price for ammonia (NH_3) we use a value for the specific consumption of hydrogen for Fischer-Trops synthesis, of 0.177 t_{H2}/t_{NH3} [31]. The cost of the electricity needed

for the synthesis is estimated at 30 €/t_{NH3} [31]. Fischer-Trops synthesis produces heat, which can be sold as district heating for 12 €/t_{NH3} [31]. Using a lower heating value of 5.17 MWh/t_{NH3} [34], the price of ammonia can be calculated. Table 6 shows the price of ammonia in countries surrounding the Baltic sea.

Country	**€/MWh$_{NH3}$**
Sweden	130.1
Finland	131.2
Denmark	141.8
Poland	173.6
Germany	175.8
Baltic countries	200.2
Russia	226.7

Table 6: Price estimate of ammonia in € per MWh, around the Baltic sea.

In the model in Section 3.1, we also allow for the purchase of fuels from the market, since in some areas it might not be suitable to construct local production facilities. Green ammonia average price data for the month of April 2024 is available from [35]. This price data is for green ammonia shipped to northwestern Europe from the US, Canada, and the Middle East. Using the average exchange rate from USD to € from 2024 [36] and the lower heating value of 5.17 kWh/kg [34], an average price for green ammonia from the global market can be calculated. Thus, the market price for ammonia is 177.96 €/MWh. It is assumed that the cost of shipping is included in this price. Currently, there is no real global market for hydrogen. Thus, if hydrogen is needed in a port, it has to be produced locally.

However, if we produce and use synthetic fuels instead of burning HFO, we do not have to purchase any HFO. This price reduction has to be taken into account. During the year of 2023 the average HFO price in northwestern Europe was 416.1 €/t [37]. Converting this to euros per MWh yields 38.42 €/MWh. If a MWh of a synthetic fuel is produced, its price is reduced by 38.42 €. Table 7 shows the final synfuel prices. For port clusters that are in several countries, the number of ports per country, and the cluster center will be used as a tie breaker to determine the price.

Country	**€/MWh$_{H2}$ (produced)**	**€/MWh$_{NH3}$ (produced)**	**€/MWh$_{NH3}$ (purchased)**
Sweden	72.6	91.7	139.5
Finland	73.5	92.8	139.5
Denmark	82.8	103.4	139.5
Poland	110.7	135.2	139.5
Germany	112.6	137.3	139.5
Baltic countries	134.0	161.8	139.5
Russia	157.2	188.3	139.5

Table 7: Synthetic fuel price table with prices relative to the price of HFO.

3.5.3 Other parameter values

The emission parameter α is determined by considering well-to-wake (WTW) emissions. WTW emissions consider the whole lifecycle of the fossil fuel. We consider CO_2 equivalent emissions (CO_2e), which take into account other emissions than just carbon dioxide such as methane and nitrogen oxides. For HFO, the best case scenario is that burning one ton of fuel emits only 3.915 tons of CO_2e emissions [38]. Combining with the lower heating value for HFO 10.83 MWh/t [34], burning HFO emits 0.3615 t_{CO2e}/MWh. However, while using a fuel cell to produce power from ammonia or hydrogen yields no emissions, producing these fuels in a renewable way still has some emissions. In the EU, regulations state that for a fuel to be called renewable, the lifetime emissions has to be below a certain threshold [39]. For ammonia and hydrogen, this value is 0.1014 t_{CO2e}/MWh. This value is the "worst case" emissions that can be emitted while still classifying the fuel as renewable. Thus, the emission parameter α is determined by the emissions that are not emitted by switching from HFO, and from the lifetime emissions that are emitted by hydrogen or ammonia. The value for α is then 0.2601 t_{CO2e}/MWh.

The parameter z determines the maximum allowed energy amount needed for a voyage that hydrogen can serve. In reality it is more complicated than this but for simplicity's sake the constraint is imposed in this way. Based on a report by [40], we assume that z is 500 MWh.

The parameter β_k^p is the minimum allowed production rate for fuel k, if fuel k is produced at a specific port. This is set to a value that will capture investor willingness, i.e., a production rate too low would not get any investors. This is set to 10950 MWh/year.

The efficiency parameter μ determines how much more efficient a fuel cell is compared to a traditional ICE. The efficiency factor is assumed to be 0.71, which means a fuel cell equipped ship would only need 0.71 times of the energy that a traditional ship would need. Table 8 shows these parameters.

Parameter	Value	Source
α	0.2601 t_{CO2e}/MWh	[38, 34]
z	500 MWh	[40]
β_k^p	10950 MWh/year	Assumed
μ	0.71	Assumed

Table 8: Parameter values and their sources.

4 Results

In this section, we first compare the performance of the different multiobjective methods. Then, we present the solutions that the model gives. Using these results, the core indices are calculated for the ports. Finally, a thorough sensitivity analysis is performed. The model is implemented in Python using Gurobi version 11.0.1 [41] as the solver, with an optimality gap of 0.01%. The computer used is a laptop with a 12th Gen Intel(R) Core(TM) i7-1265U, and 16 GB of RAM.

4.1 Multiobjective method comparison

Since computing the complete Pareto optimal set is not reasonable for a model of this size, we are interested in computing reasonably sized and evenly spaced subsets of the complete Pareto optimal set. Figure 12 shows how the different multiobjective methods from Section 2.5 compare when computing a small subset of the complete Pareto optimal set.

We notice that the weighted Tchebycheff method (Figure 12b) and the weighting method (Figure 12c) perform poorly when only solving for a small amount of Pareto optimal solutions. The Tchebycheff method does not find evenly distributed points, they are instead more concentrated in the upper end, even though the weights are evenly distributed. The same can be said for the weighting method, but since the weighting method can only find points on the convex hull of the feasible objective region, we notice large gaps. Thus, both of these methods are not well suited for the task at hand.

Both the ε-constraint method (Figure 12a) and the Boxing method (Figure 12d) perform well in the sense that the individual points are evenly distributed. The boxing method yields 25 Pareto optimal solutions since the desired amount of solutions cannot be directly input into the method. Due to the even spacing for the solutions given by the ε-constraint method, it is chosen as the default multiobjective method for further analysis. If the Pareto optimal set was less like a straight line, the Boxing method would probably be preferred since the distances between points can change depending on the angle between them.

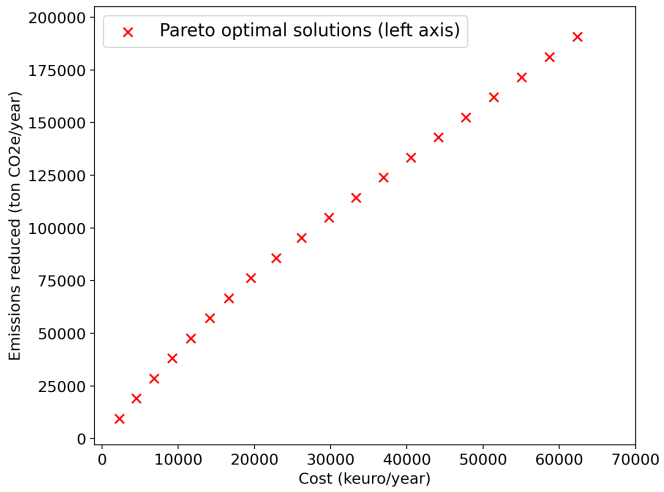

(a) 20 Pareto optimal solutions using the ε-**constraint** method.

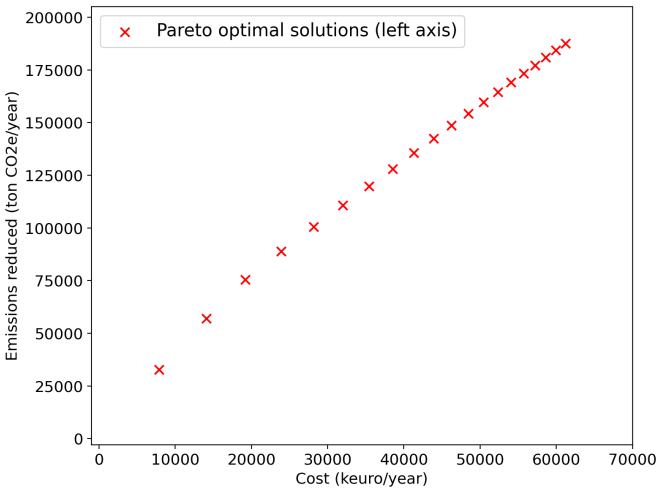

(b) 20 Pareto optimal solutions using the weighted **Tchebycheff** method.

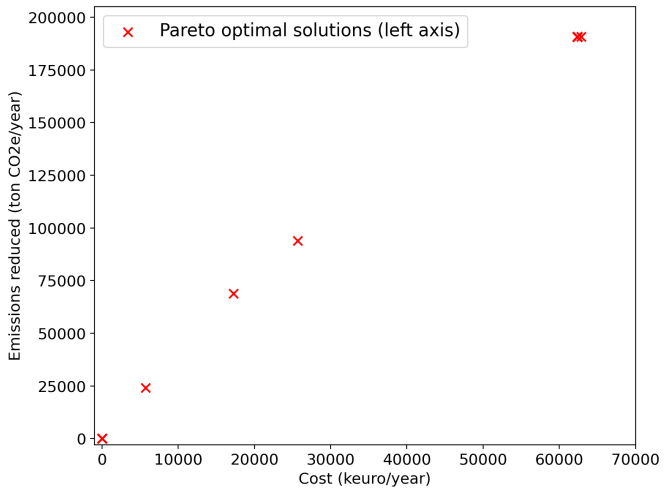

(c) 20 Pareto optimal solutions using the **weighting** method.

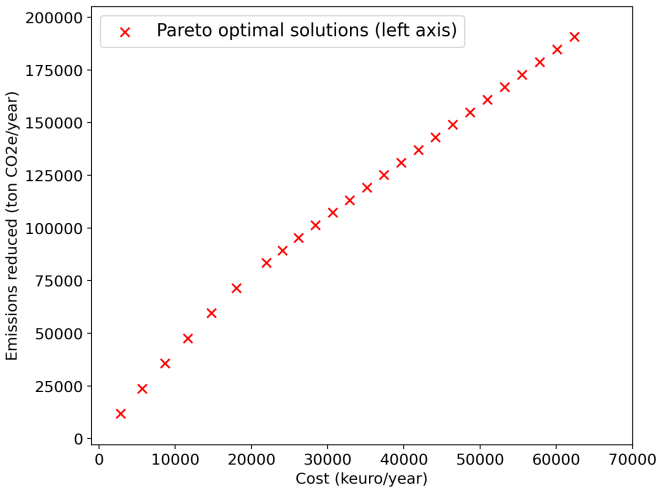

(d) 25 Pareto optimal solutions using the **Boxing** method.

Figure 12: Pareto optimal solutions found using different multiobjective methods.

4.2 Model solution

Figure (13) shows a thousand Pareto optimal solutions in red, and the specific cost of emission reduction for every solution in blue. The specific cost of emission reduction measures how much you pay per ton of reduced emissions, for every solution. Two specific solutions, A and B are highlighted, and will be discussed further in a later stage. We notice that the specific cost of emission reduction (blue line) does not behave nicely at the lower end of the graph. This is because, while the corresponding solutions are mathematically optimal, the overall cost is so low that the minimum production constraint really dictate the solutions. For example, in the top left corner of Figure 13, we notice that the specific cost of emissions peaks when the cost is close to zero. This is because all those solutions are only comprised of buying ammonia

from the market since producing over the minimum production rate is too expensive. Ignoring these solutions only comprising of buying ammonia, the specific cost of emissions lies between 230 and 330 €/ton. The specific cost of emission reduction given by the model can be compared to the European emission trading system (ETS) price which during the year 2023 averaged at 85.3 €/ton, and peaked at over 100 €/ton [42]. During the year 2023, maritime shipping emissions were not included in the ETS. However, from 2024 onward it is included [43]. It is estimated that the ETS price will reach almost 200 €/ton in 2035 [44]. This estimated ETS price is then not far from the lower end estimated by the model.

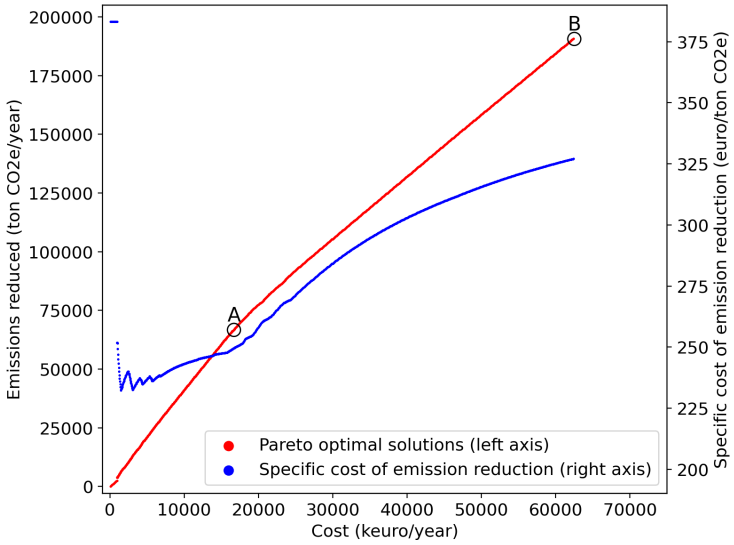

Figure 13: Figure showing a thousand Pareto optimal solutions.

Let us examine solution A (shown in Figure 13). Figure 14 shows where, and how much of each fuel is produced. As is to be expected, for this solution, optimal production locations are concentrated to the countries with the least expensive synthetic fuels. The production centers from west to east are Aarhus and Copenhagen in Denmark, Gothenburg and Gävle in Sweden, and the Turku region, Helsinki and Kotka in Finland. The three westernmost ports have a quite even split between producing ammonia and hydrogen, while the four easternmost ports are predominantly producing ammonia. This indicates that in the western Baltic sea there is a lot of shorter voyages being done that are suitable to Hydrogen fueling, while in the east the voyages are on average longer which is not suitable to hydrogen, and needs ammonia instead. In this solution no ammonia is needed to be bought. This solution has a specific cost of emissions of around 250 €/ton.

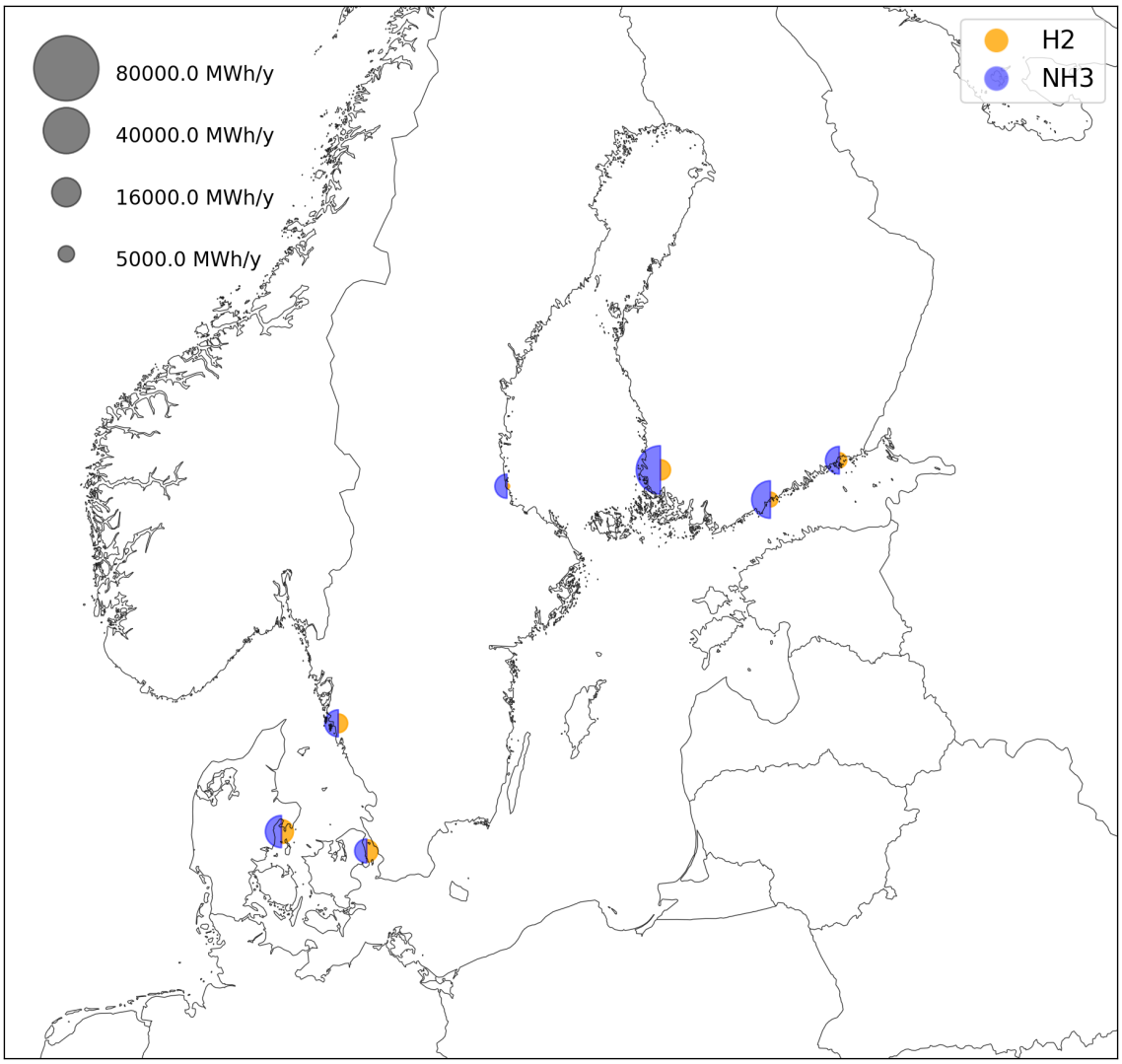

Figure 14: Map showing production amounts and locations for solution A. Production amount indicated by the size of the half circle.

We can also study a solution at the top of the cost range to see how it compares. We study solution B in Figure 13. This solution has a specific cost of emission reduction of around 325 €/ton. Figure 15 shows this solution. Many of the ports included in this solution were also present in the previously shown solution, which is to be expected since they are comparatively inexpensive. Five port clusters in the south have been added to this solution, the East Frisian peninsula, the Bremen region, and the Hamburg region in Germany, and the Szczecin region and Gdansk region in Poland. For this purpose Germany is considered a country bordering the Baltic sea and thus the western ports in Germany are included. The Bremen and Hamburg regions are the largest producers of both ammonia and hydrogen, which reflects on Germany's status as the largest economy in Europe.

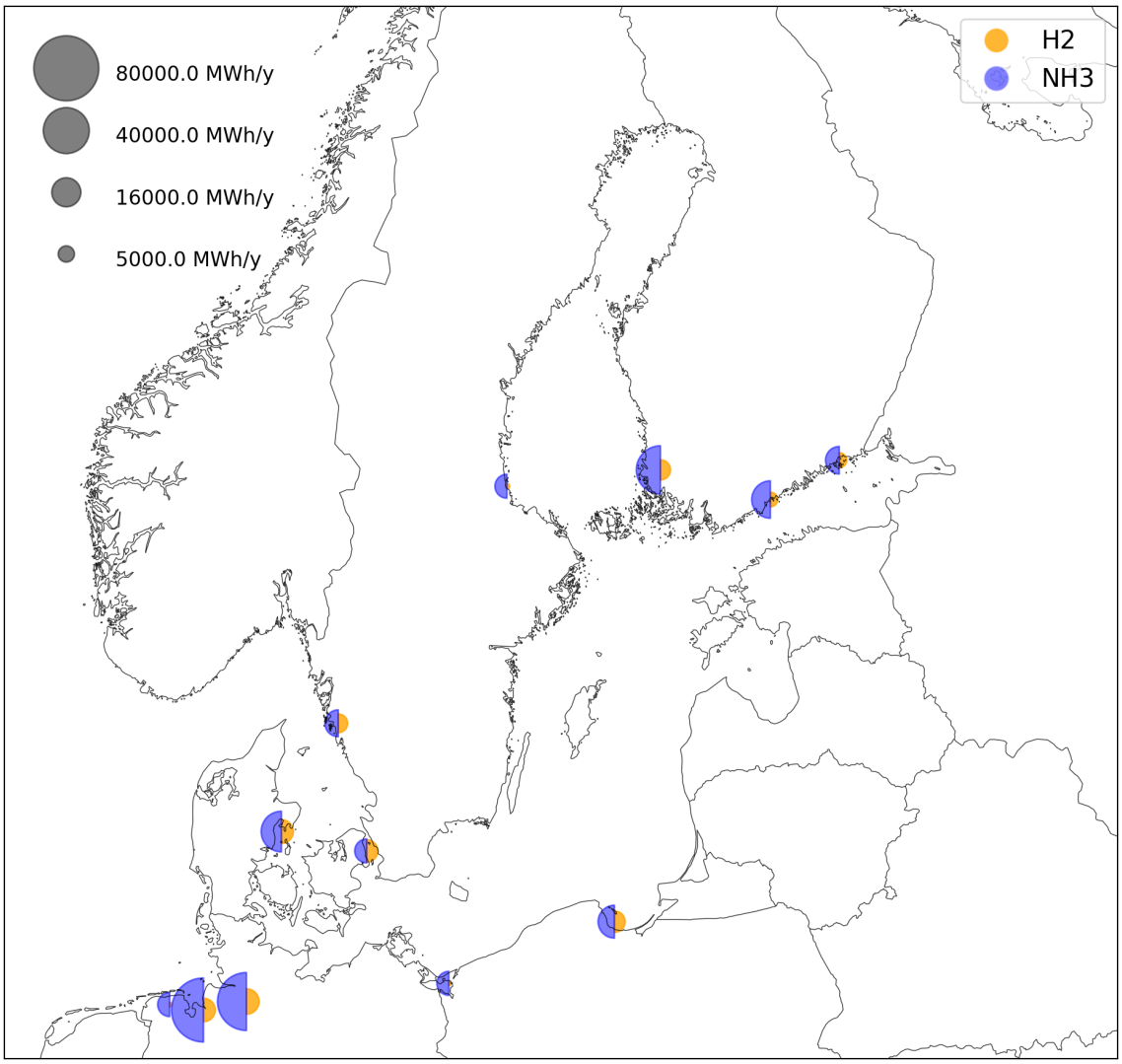

Figure 15: Map showing production amounts and locations. Solution B is shown.

However, in this solution, ammonia is also purchased to several ports. Figure 16 shows were ammonia is purchased. The locations were ammonia is purchased to can be divided into two groups. One is where the estimated price of producing ammonia locally is more than the market price, such as the Baltic countries and Russia. The other is where the minimum production amount for ammonia cannot be achieved, and thus ammonia has to be purchased. Such ports can be observed in Germany and Sweden. The three most notable ports, where ammonia is purchased, are Tallinn in Estonia, Riga in Latvia, and Klaipėda in Lithuania.

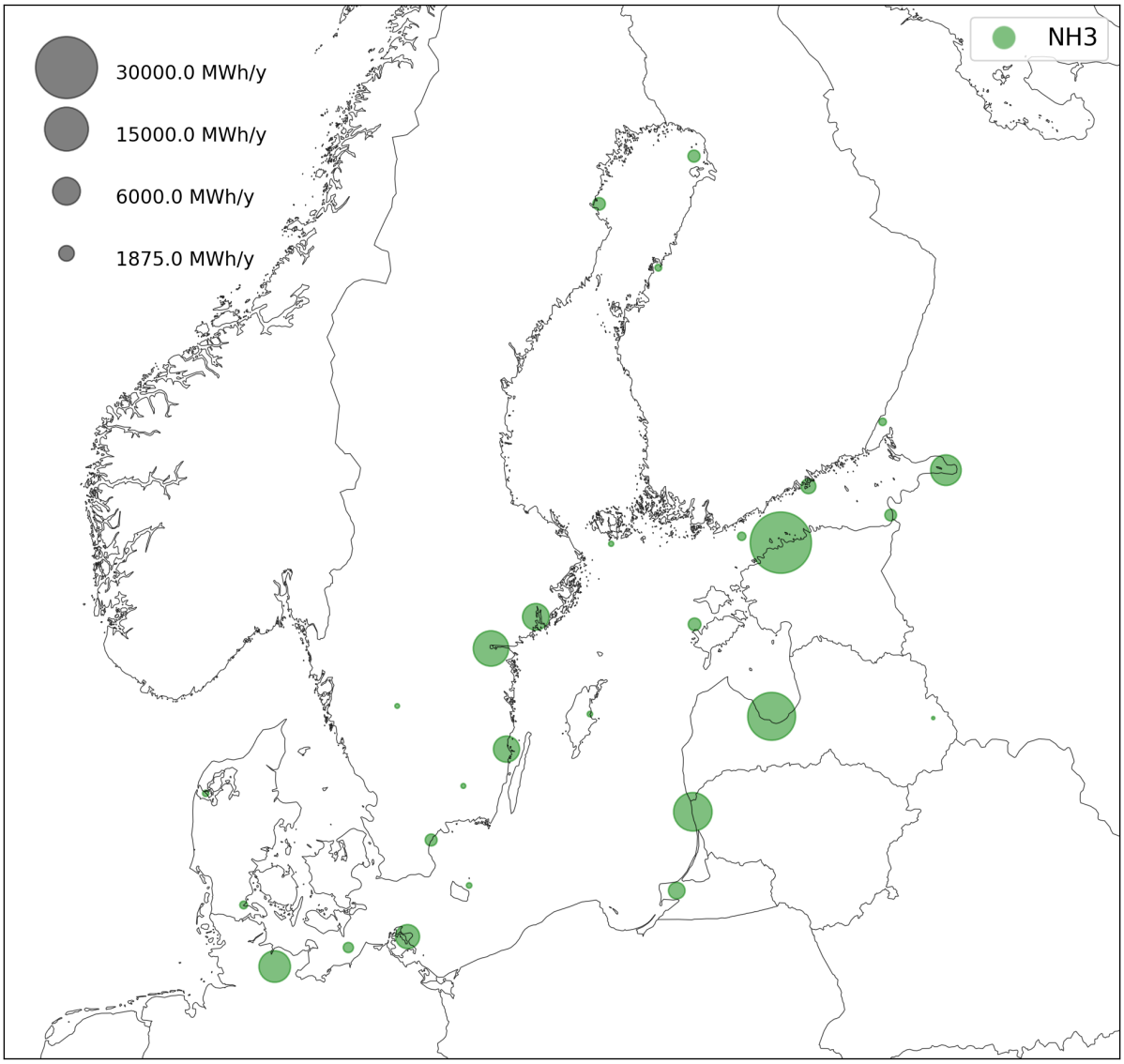

Figure 16: Map showing ammonia purchase amounts and locations. The most expensive solution is shown.

4.3 CPU runtimes

We can also study how the CPU runtimes differ when varying the number of Pareto optimal solutions, and the optimality gap. When varying the number of Pareto optimal solutions, the standard optimality gap of 10^{-4} is used, and when varying the optimality gap, we find 20 Pareto optimal solutions. Table 9 shows how the CPU runtimes vary. When varying the desired number of Pareto optimal solutions, the runtime increases almost linearly, which is to be expected. However, when decreasing the optimality gap the runtime increases non linearly. When varying the optimality gap, the core indices

and the optimal production amounts do not change beyond the variance allowed for by the optimality gap.

Number of Pareto optimal solutions	Solution time (s)	Average time per solution (s)
20	8	0.40
200	79	0.40
1000	387	0.39
Optimality gap	**Solution time (s)**	**Average time per solution (s)**
10^{-4}	8	0.40
10^{-5}	20	1.00
10^{-6}	169	8.45
10^{-7}	337	16.9

Table 9: CPU runtime for different number of Pareto optimal solutions and different optimality gaps.

4.4 Port core indices

We use the core index (CI) defined in Section 3.4 to condense the information from all available Pareto optimal solutions. The Pareto optimal solutions used to calculate the core indices are seen in Figure 13. Figure 17 and Table 10 shows the core indices for the Baltic sea ports. Ports not in this list have core indices of zero. The ports with core indices of zero are infeasible with respect to the constraints of the model, or ports were it is cheaper to buy ammonia instead of producing. This means that we can recommend against them. We see that the ports with the highest core indices are in countries with low cost of hydrogen, Sweden and Finland. The core indices are in general very similar for hydrogen and ammonia at a given port, with the notable exception of Hamburg, where the hydrogen core index is significantly larger. Table 10 also shows the maximum amount of synthetic fuels that could be produced in each port, as well as the specific cost of emissions for that port if all the synthetic fuel is used for ships. From the original list of 173 ports, 12 areas have been identified to have a non zero core index, which is a large reduction.

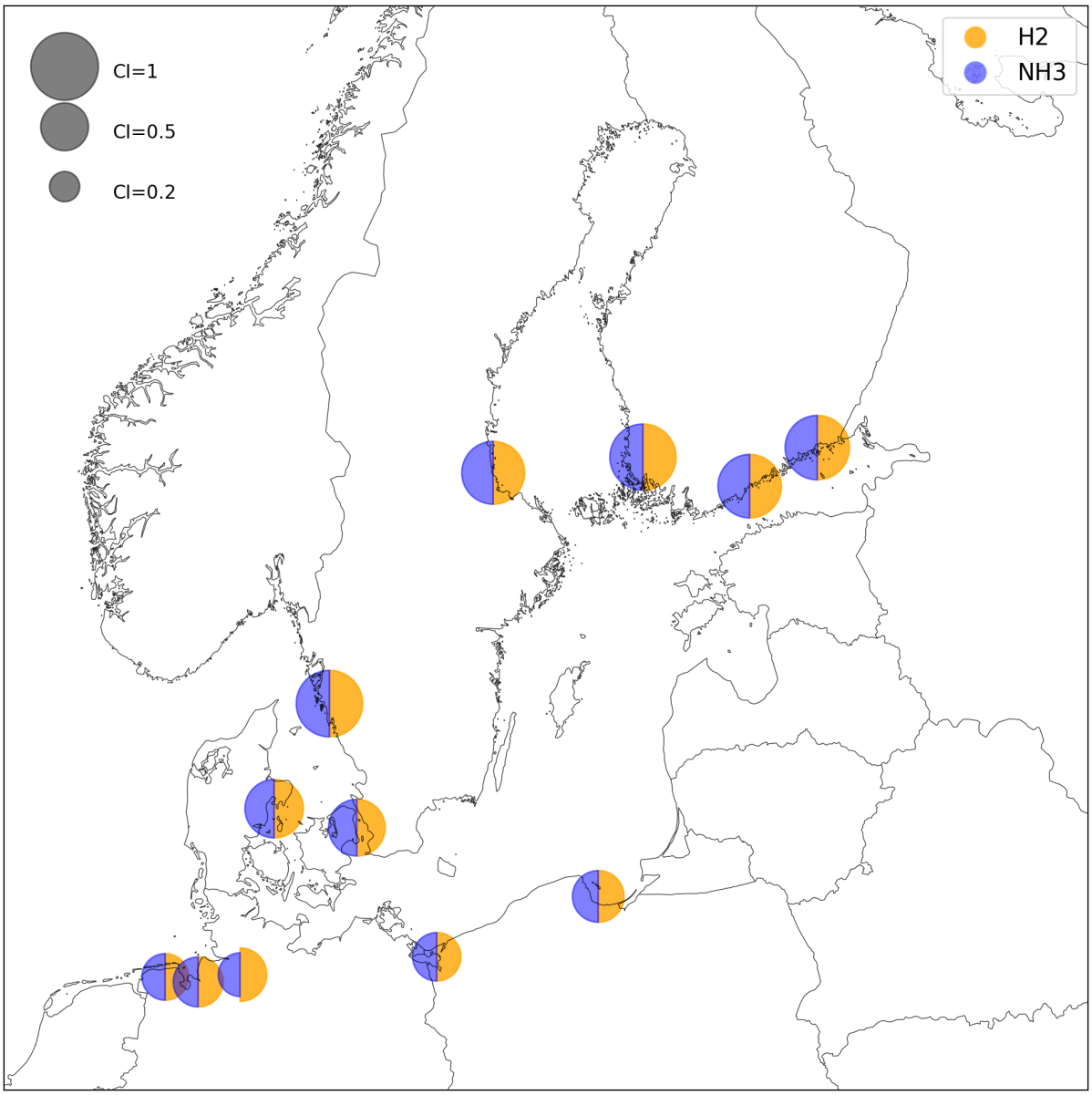

Figure 17: Map showing the core indices calculated from a thousand Pareto optimal solutions.

Cluster id	Place name	CI H2	CI NH3	Capacity H2 (MWh/y)	Capacity NH3 (MWh/y)	Specific cost of emission reduction (€/ton)
14	Gothenburg	0.96	0.97	6605	13700	234.7
15	Turku	0.96	0.96	7690	44096	246.9
30	Kotka	0.91	0.91	4180	14398	242.8
1	Helsinki	0.88	0.88	3987	26483	247.8
18	Gävle	0.86	0.86	566	10952	249.2
9	Aarhus	0.75	0.75	10670	31391	269.5
4	Copenhagen	0.70	0.70	9382	10954	257.8
0	Hamburg	0.62	0.42	12206	63468	366.2
3	Gdansk	0.58	0.58	8602	20474	351.4
37	Bremen	0.55	0.55	10398	77597	369.1
26	Szczecin	0.51	0.51	333	10964	369.3
11	East Frisian peninsula	0.48	0.48	373	10954	374.9

Table 10: Core indices for the port clusters in the Baltic sea, calculated from a thousand Pareto optimal solutions.

It is worth noting that the core index is not simply a measure of the specific cost of emissions. We see in Table 10 that ports with low specific cost of emissions in general have high core indices and vice versa. However, in this case, a high core index seems to mean that that port has either a high capacity, low specific cost of emissions, or a combination of the two. E.g. Turku has a higher specific cost of emissions compared to Gävle, but the core indices for Turku are higher. Turku has a significantly higher production capacity compared to Gävle.

We can also study how the core indices are affected by the number of Pareto optimal solutions used. Table 11 shows the core indices calculated with 1000, 200, and 20 Pareto optimal solutions. The maximum absolute deviation observed is 0.048. This is still relatively large. If we ignore the indices from only 20 Pareto optimal solutions, the maximum absolute deviation is only 0.009. Thus, computing the core indices with only 200 evenly distributed Pareto optimal solutions is reasonable. Unless otherwise stated, core indices are computed from 200 Pareto optimal solutions.

	1000 Solutions		200 Solutions		20 Solutions	
Cluster id	**CI H2**	**CI NH3**	**CI H2**	**CI NH3**	**CI H2**	**CI NH3**
14	0.963	0.968	0.970	0.975	0.900	0.950
15	0.960	0.960	0.960	0.960	1.000	1.000
30	0.907	0.907	0.910	0.910	0.950	0.950
1	0.882	0.882	0.880	0.880	0.900	0.900
18	0.864	0.864	0.870	0.870	0.900	0.900
9	0.747	0.747	0.750	0.750	0.750	0.750
4	0.702	0.702	0.705	0.705	0.750	0.750
0	0.623	0.417	0.625	0.420	0.650	0.450
3	0.583	0.583	0.585	0.585	0.600	0.600
37	0.545	0.545	0.545	0.545	0.550	0.550
26	0.511	0.512	0.520	0.520	0.550	0.550
11	0.475	0.475	0.475	0.475	0.500	0.500

Table 11: Comparison between the core indices for different number of Pareto optimal solutions.

4.5 Sensitivity analysis

To validate the model, sensitivity analysis is needed. We analyze the model when varying the cost of hydrogen, which is probably the parameter that will vary the most in the real world compared to our estimates. The minimum allowable production rate is also varied, since it is a parameter that is difficult to realistically estimate

4.5.1 Cost of hydrogen

The cost of hydrogen is likely to vary in the real world. The cost of green hydrogen also directly influences the cost of ammonia. We will study how the core indices, as well as the specific cost of emission reduction (€/t_{CO2e}) are affected by changes in the price of hydrogen. We study the impact of a 10% and a 50% increase, as well as a 10% decrease in the cost of hydrogen. The price of buying ammonia from the market is not affected

Increasing the cost of hydrogen by 10% or 50% increases the relative price compared to HFO by more than 10% or 50% respectively. This is also true for ammonia, the price of which is dependant on the price of hydrogen. Table 12 shows the new fuel prices.

Country	Base		10% increase		50% increase	
	H2	NH3	H2	NH3	H2	NH3
Sweden	72.6	91.7	83.7	104.4	128.1	155.0
Finland	73.5	92.8	84.7	105.5	129.5	156.6
Denmark	82.8	103.4	94.9	117.2	143.4	172.5
Poland	110.7	135.2	125.6	152.2	185.3	220.3
Germany	112.6	137.3	127.7	154.6	188.0	223.5
Baltic countries	134.0	161.8	151.2	181.4	220.1	260.1
Russia	157.2	188.3	176.8	210.6	255.0	299.9

Table 12: Hydrogen and ammonia prices relative to HFO, in €/MWh.

Figure 18 shows 20 Pareto optimal solutions, for a hydrogen price increase of 10% and 50%. We notice in Figure 18a that the specific cost of emissions is slighly higher than the base case. However, in Figure 18b, the specific cost of emissions graph is horizontal and constant. This is because with the 50% increase in the cost of hydrogen, all the solutions only consist of buying ammonia from the market.

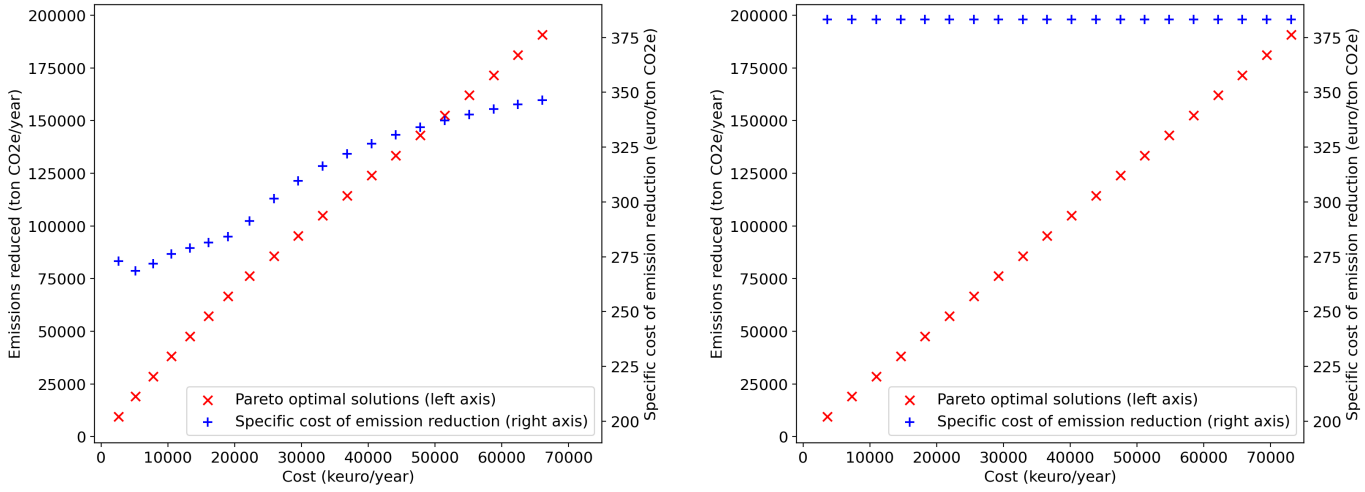

(a) 20 Pareto optimal solutions with a 10% increase in the cost of hydrogen.

(b) 20 Pareto optimal solutions with a 50% increase in the cost of hydrogen.

Figure 18: Comparison between Pareto optimal solutions for different prices for hydrogen.

Figure 19 shows the core indices with price increase of 10%. Since the model chooses to not produce anything with the 50% increase in the price all the core indices are zero in that case. We see that many ports see no apparent change in their core indices, except for ports in Germany and Poland. German and Polish ports all have core indices of zero, except for Bremen in Germany where the hydrogen core index is nonzero. With the increase in the price of hydrogen, it is cheaper to buy ammonia in Poland and Germany. With no ammonia production, there is not enough hydrogen demand on its own to get over the minimum production amount, except for in Bremen.

The production and purchase amounts for the most expensive solution are shown in Appendix B in Tables B1 and B2.

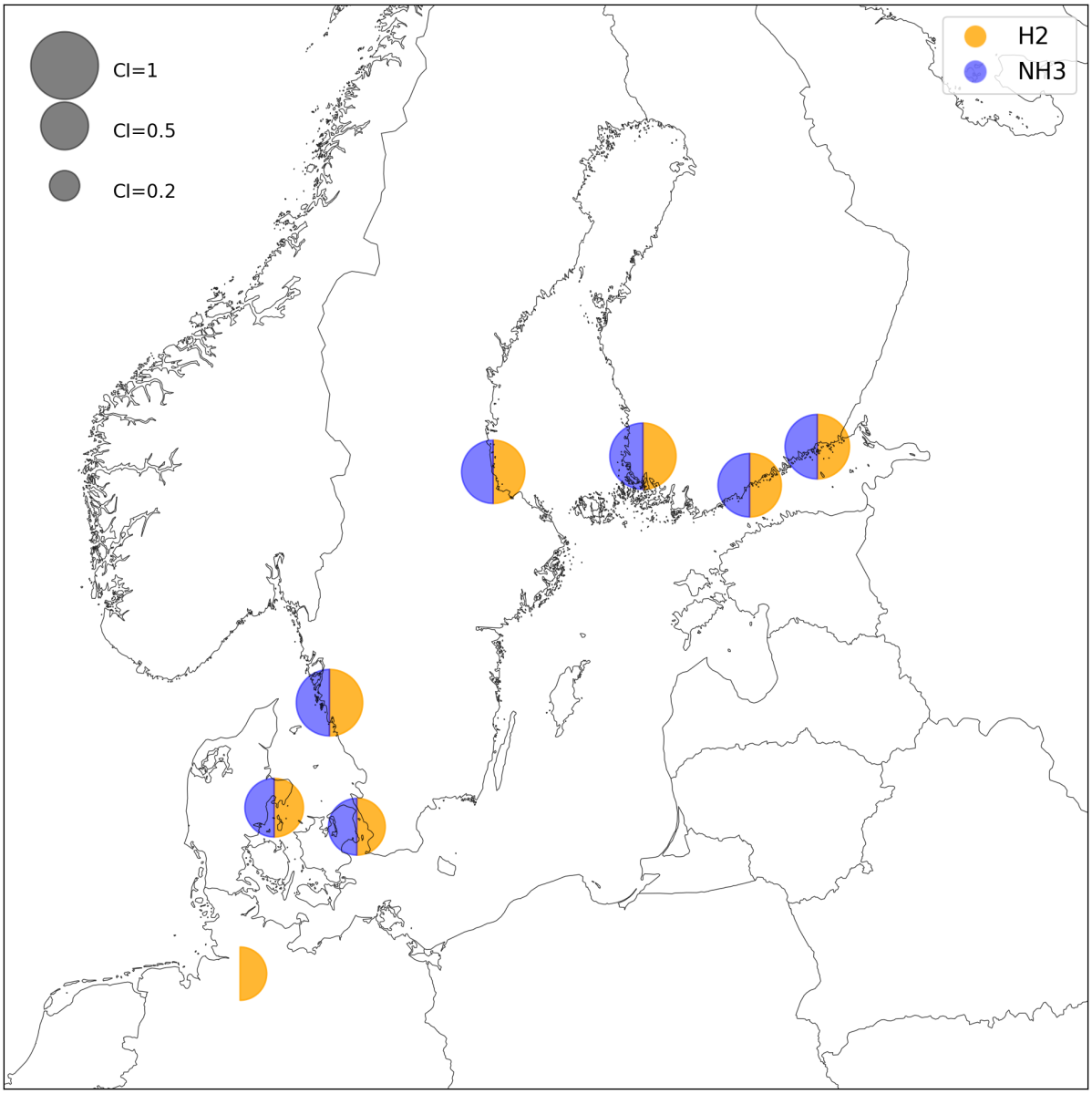

Figure 19: Map showing the core indices with the price of hydrogen increased by 10%, calculated from 200 Pareto optimal solutions.

Next, we reduce the price of hydrogen by 10%. Table 13 shows these new prices compared to the base prices.

Country	Base		10% decrease	
	H2	NH3	H2	NH3
Sweden	72.6	91.7	61.5	79.0
Finland	73.5	92.8	62.3	80.0
Denmark	82.8	103.4	70.7	89.5
Poland	110.7	135.2	95.8	118.2
Germany	112.6	137.3	97.5	120.1
Baltic countries	134.0	161.8	116.7	142.1
Russia	157.2	188.3	137.6	166.0

Table 13: Ammonia and hydrogen prices, relative to HFO, with a 10% decrease in the price of hydrogen. Given in €/MWh.

Figure 20 shows 20 Pareto optimal solutions with the decreased price. No large differences compared to the base case shown in Figure 12a is observed. Figure 21 shows the core indices with the decreased fuel prices. Here, the biggest difference is that Tallinn, Estonia, and Riga, Latvia, now have non zero core indices for both hydrogen and ammonia. The production and purchase amounts for the most expensive solution are shown in Appendix B in Tables B3 and B4.

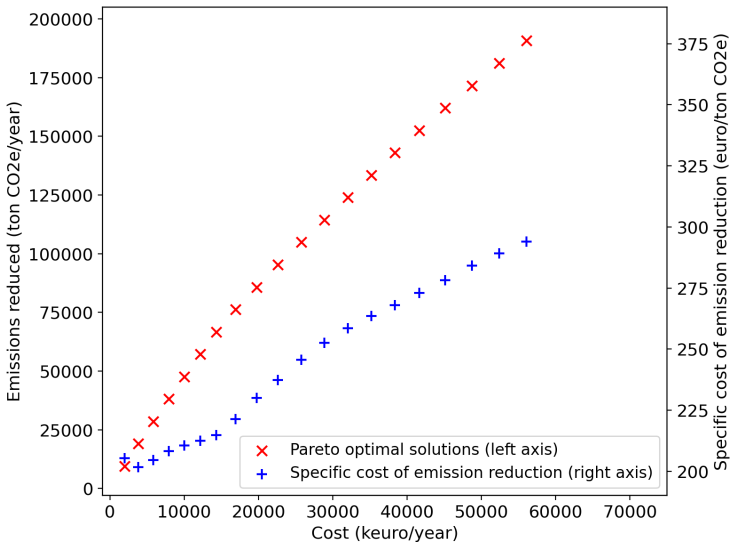

Figure 20: 20 Pareto optimal solutions with the decreased prices given in Table 13.

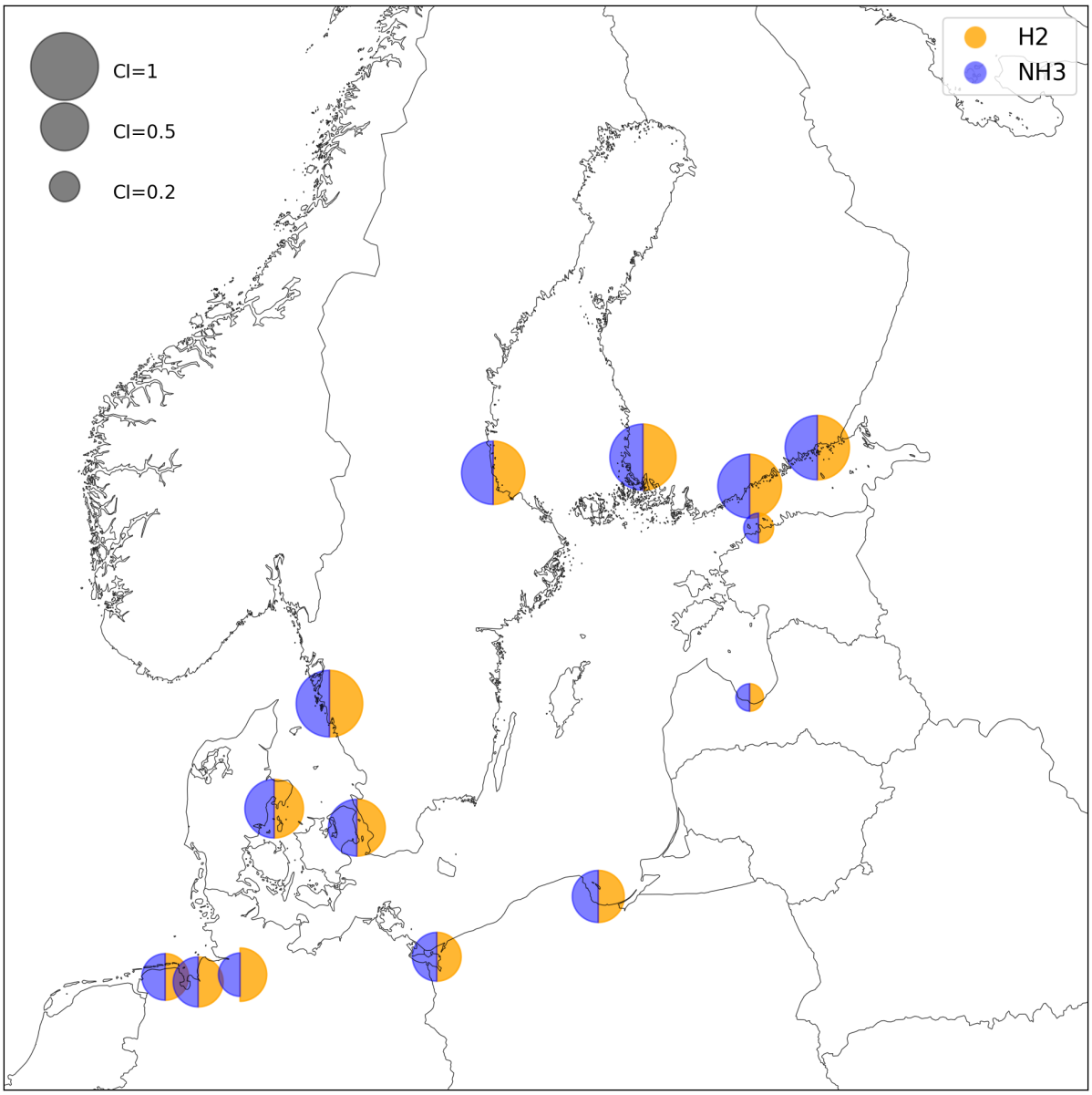

Figure 21: Map showing the core indices with the price of hydrogen decreased by 10 %, calculated from 200 Pareto optimal solutions.

Ports, where the price of producing ammonia is close to the market price of ammonia are somewhat sensitive to changes in the price of hydrogen (and ammonia). We see that a 10% increase in the price of hydrogen leads to it not being feasible to produce fuels in Germany (except Bremen) and Poland. On the other hand, decreasing the cost of hydrogen makes it somewhat feasible to produce in Tallinn and Riga indicated by their nonzero, but still small core index. A potential decision maker needs to carefully consider these prices. On the other hand, producing in inexpensive countries is an easier choice, indicated by their high core indices.

4.5.2 Minimum production amount

The model might be sensitive to the minimum production rate, since there are probably ports with favourable prices that do not quite have enough outgoing traffic to reach the minimum production amount. We study what happens if we lower the minimum production rate to 5000 MWh/y and to 1 MWh/year from the base case of 10950 MWh/y.

Figure 22 shows 20 Pareto optimal solutions, with a minimum production rate of 5000 MWh/y and 1 MWh/y respectively. We notice that the specific cost of emissions (blue crosses) is lower in Figure 22b. This is because the minimum production rate of 1 MWh/year is so low that all voyages that could use hydrogen are using it, and hydrogen has the lowest price.

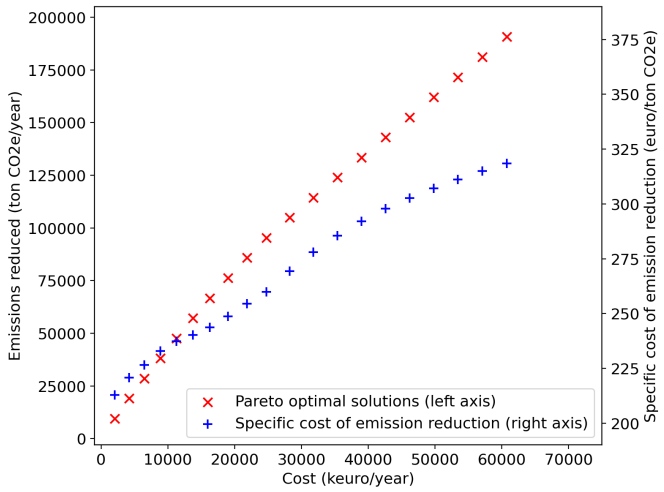

(a) 20 Pareto optimal solutions with a minimum production rate of 5000 MWh/y.

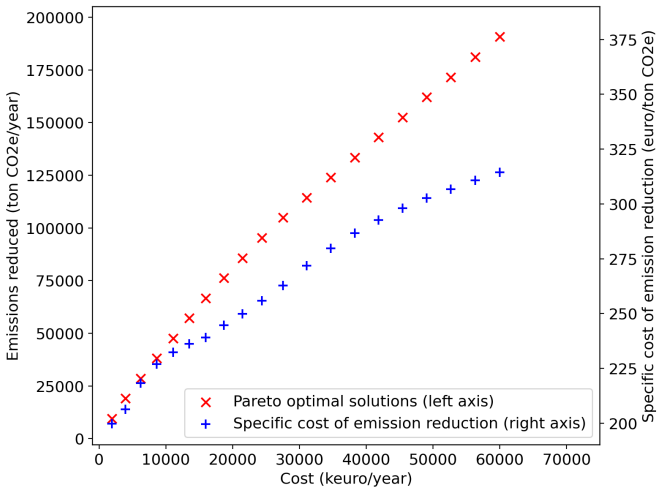

(b) 20 Pareto optimal solutions with a minimum production rate of 1 MWh/y.

Figure 22: Comparison between Pareto optimal solutions for different minimum production rates.

Figure 23 shows the core indices for different minimum production rates. Figure 23a is in many ways similar to Figure 17, with the notable addition that four new ports have been added with a nonzero hydrogen core index. These ports are, from west to east the Kiel area in Germany, Klaipėda in Lithuania, Riga in Latvia, and Tallinn in Estonia. The German and Danish ports have higher hydrogen core indices compared to the ammonia core indices. Otherwise, the ammonia core index is not heavily affected by the lowering of the minimum production constraint. The production and purchase amounts for the most expensive solution are shown in Appendix B in Tables B5 and B6.

Figure 23b shows the core indices when the minimum production rate is set to 1 MWh/y. For the ammonia core indices there is not a large difference, except one new port cluster in northern Sweden. The largest difference however, is that hydrogen has a relatively large core index in almost every port. Since this instance has practically no

minimum production amount, and hydrogen is less expensive than ammonia, hydrogen in produced in small quantities almost everywhere. Ports with an ammonia core index of zero can mean two things, either, no routes long enough to not be able to be served by the less expensive hydrogen, or buying ammonia from the market is cheaper than producing locally, such as e.g. the Baltic countries. The production and purchase amounts for the most expensive solution are shown in Appendix B in Tables B7 and B8.

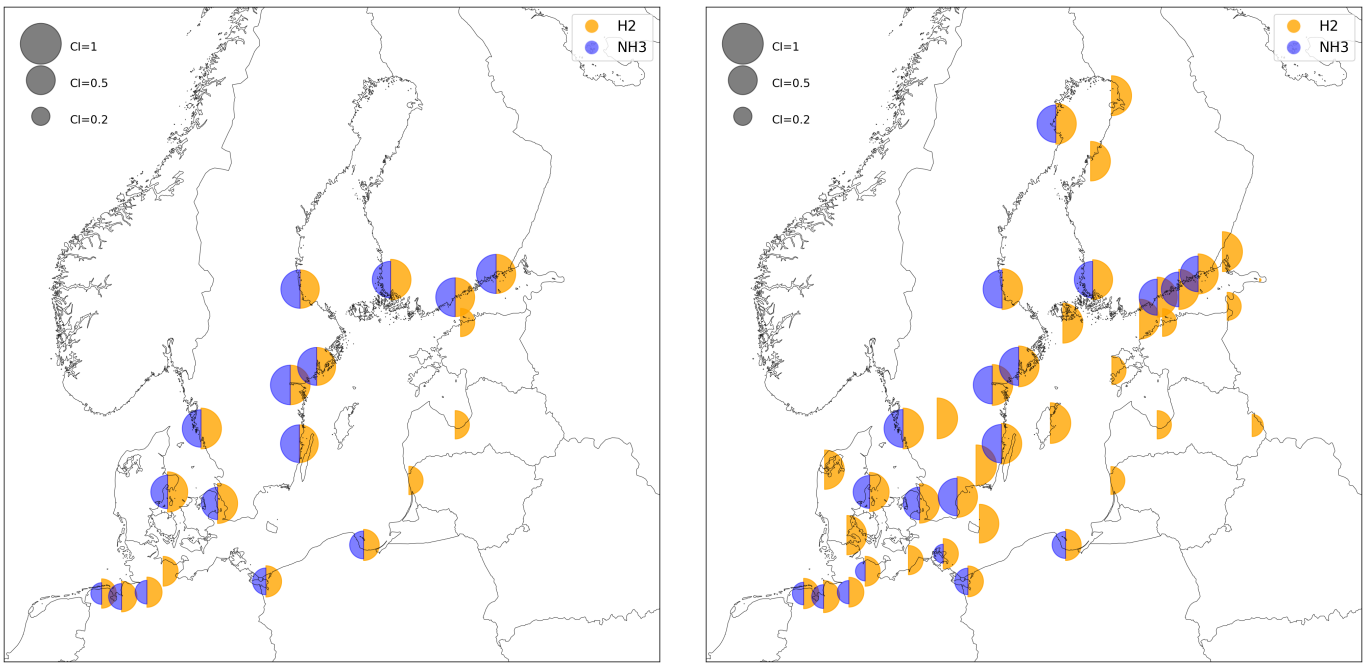

(a) Core indices with a minimum production rate of 5000 MWh/y.

(b) Core indices with a minimum production rate of 1 MWh/y.

Figure 23: Comparison between core indices for different minimum production rates. Core indices calculated from 200 Pareto optimal solutions.

The ammonia core indices are, in general, not heavily impacted by varying the minimum production rate. The hydrogen core indices are in general more sensitive. However, if we ignore the unrealistic scenario of the minimum production rate being 1 MWh/y, the hydrogen core indices are not heavily impacted. Even when halving the original minimum production rate, the core indices that were above zero originally did mostly stay the same. Four new ports had a hydrogen core index above zero, which can be categorized into ports with potential for hydrogen production, if a smaller minimum production rate is acceptable, i.e., if small investments are possible from an investors point of view.

5 Conclusions

Maritime shipping accounts for almost 3% of yearly global greenhouse gas emissions. One potential way to reduce these emissions is to switch from burning oil to renewable synthetic fuels. Hydrogen and ammonia can be produced in a renewable way, and can be fed into a fuel cell to directly generate electricity to power a ship. Ammonia can also be burned in engines like traditional marine fuels, aiding the potential switch.

A mixed-integer linear program for identifying decarbonized bunkering options in the Baltic sea was developed and implemented. The model aims to maximize a decrease in emissions while minimizing the associated costs. A price model for hydrogen and ammonia in countries surrounding the Baltic sea was developed to be used with the optimization model. Historical ship data from the year 2023 for voyages was used to be able to run the model. A brief comparison between multiobjective methods was also performed.

The hydrogen prices were estimated to be the lowest in Sweden and Finland, closely followed by Denmark. Poland and Germany are estimated to have medium priced hydrogen, while the Baltic countries and Russia have expensive hydrogen. The cost of hydrogen is mostly determined by the cost of wind energy in the different countries. The cost of hydrogen is the largest part of the cost of green ammonia, since green ammonia is produced from green hydrogen.

Ship voyage data from 2023 was used. All ports present in the data were clustered into 40 appropriately sized clusters. The different ships in the data were grouped into six different groups based on the size of the vessel and ship type. Routes were then defined as from one port cluster to another, for every ship group. The data consisted of around 5000 individual routes.

The concept of robust ports was introduced. A robust port is a port where producing ammonia or hydrogen is optimal, regardless of the preference between maximizing the decrease in emissions and minimizing costs. The robustness of a port is measured by its core index which takes a value between zero and one. A value of one means that a fuel is produced in that port in every Pareto optimal solution, while a value of zero indicates that a fuel is never produced in that port. The ports with the highest core indices, in order, were Gotheburg, Turku, Kotka, Helsinki, and Gävle. Seven other port clusters also had non zero core indices. These ports are such, that producing synthetic fuels for bunkering is optimal. The core index seems to be a suitable metric, since it takes into account both the specific cost of emissions, as well as the capacity.

Sensitivity analysis on the model was performed, first by varying the cost of hydrogen, which will likely vary in the real world. Since ammonia needs to be produced from hydrogen, changing the price of hydrogen affects the price of ammonia as well. What was found from this is ports where the cost of producing ammonia is close to the market price, which did not change during the sensitivity analysis, were sensitive to the changes in the cost of hydrogen. If the price of producing ammonia increased above the market price it was no longer optimal to produce there. Similarly, if the price of producing dropped below the market price, it could become optimal to produce. However, ports where hydrogen prices were very low or very high, were not impacted by this. Thus, a potential decision maker has to be careful considering

prices and price estimates regarding producing and purchasing ammonia.

Then, sensitivity analysis on how varying the minimum allowable production rate impacted the core indices was done. The minimum production rate is enforced to limit producing small amounts scattered everywhere, and instead trying to concentrate production and bunkering facilities, since it is assumed that investors are not keen on too small projects. When halving the minimum production rate, only four additional ports became feasible for hydrogen production, and none for ammonia. This is a good sign since estimating a realistic minimum production rate is difficult. Among these newly added ports, one was in each Baltic country. Two of which, Tallinn and Riga, also became feasible when slightly lowering the price of hydrogen. This means that Tallinn and Riga might also be feasible ports for decarbonized bunkering, since decreases in either the cost of hydrogen, or the minimum production rate has made them feasible. Better hydrogen price estimates for the Baltic countries could make this decision more certain.

One thing that has become clear is that the local hydrogen production and pricing has a large impact on feasibility of ports. Currently, it is only feasible to produce hydrogen locally, but that might need to change. If the inexpensive prices in the Nordic countries could be leveraged for production, and then those synfuels could be exported to other countries around the Baltic sea, the prices could potentially go down in the expensive areas. Lower prices would increase feasibility.

Comparing the specific cost of emission reduction gained from the model with the European emission trading system (ETS) price is difficult. During the year 2023, ETS did not include maritime shipping. During that same year the ETS price averaged around 85 €/ton, while the model ranged from 230 to 330 €/ton. While the estimates from the model are conservative, it is still a significant increase. However, due to maritime shipping being included in the system from 2024 onwards and due to the emission cap in the system decreasing every year, it is reasonable to think that the ETS price will increase in the coming years. It is estimated that the ETS price will reach almost 200 €/ton in 2035, which means the difference could be small by then.

5.1 Limitations

Current ship operators usually prefer to bunker once when the ship is in a port with inexpensive bunkering and then sail for weeks or potentially months before bunkering again. This model is not set up to reflect on these preferences. The available data was not set up in such a way that longer voyages that include several ports for a single ship could be identified. However, these preferences that current ship operators have might need to be challenged if synthetic fuels are to be used in the future. Due to the lower volumetric density, especially of hydrogen, more frequent bunkering is needed to not sacrifice carrying capacity too much.

Due to the apparent unavailability of wind PPA data in the Baltic countries, their hydrogen price estimates is thus lacking. The hydrogen price was then estimated to be the average between the Russian and Polish prices, both of which neighbor the Baltic countries. This turned out to be a somewhat sensitive price, and better price estimates would be needed to be able to make better decisions for the Baltic countries.

Currently, a green hydrogen economy does not yet fully exist. However, it is reasonable to think that this will change in the future, i.e., green hydrogen will be produced and consumed by large quantities. This means that the minimum production rate constraint imposed in this model might not make sense anymore. Producing more hydrogen than what is needed for ships in a port could be feasible since the excess hydrogen could just be sold to other sectors that need it.

5.2 Future work

Expanding the data to e.g. incorporate the North Sea would be a great addition to just the Baltic Sea. It is reasonable to assume that many ships leave the Baltic Sea for the massive ports in the Netherlands and Belgium. Also incorporating more ship types could be interesting, for example Ro-pax (roll on/roll off passenger ships) usually cover the same route all the time which could make them very suitable to synthetic fuels due to the reduced uncertainty.

Changing the model to allow for "chained" routes, and thus for refueling less often, while much more complicated, would allow for a more detailed analysis of routes. It would also allow for more realistic refueling strategies to be modeled and optimized.

The ports in the original dataset was first clustered, based on location, where the number of clusters was determined beforehand. This was done partly to make the dataset more manageable, and partly since producing synthetic fuels at a location could serve several ports if they are close enough. However, it could potentially be more realistic to cluster the ports in a better way. Perhaps, clustering the ports based on more than just location, e.g., potential production amount could make the clusters more uniform. Some form of dynamic pricing could be incorporated so that a individual port could belong to a cluster further away but with a higher price, if the original cluster does not reach the minimum production amount. This is related to the uncapacitated facility location problem, which already exists in literature.

References

[1] International Maritime Organization, "Fourth Greenhouse Gas Study 2020." https://www.imo.org/en/OurWork/Environment/Pages/Fourth-IMO-Greenhouse-Gas-Study-2020.aspx, 2020. Accessed: 2024-04-26.

[2] International Maritime Organization, "Revised GHG reduction strategy for global shipping adopted." https://www.imo.org/en/MediaCentre/PressBriefings/Pages/Revised-GHG-reduction-strategy-for-global-shipping-adopted-.aspx, 2023. Accessed: 2024-04-26.

[3] Getting to Zero Coalition, "The Next Wave Green Corridors," *Global Maritime Forum*, 2021.

[4] B. D. Brouer, C. V. Karsten, and D. Pisinger, "Optimization in liner shipping," *4OR*, vol. 15, pp. 1–35, 3 2017.

[5] International Maritime Organization, "Fourth Greenhouse Gas Study 2020 executive summary." https://wwwcdn.imo.org/localresources/en/OurWork/Environment/Documents/Fourth%20IMO%20GHG%20Study%202020%20Executive-Summary.pdf, 2020. Accessed: 2024-05-21.

[6] M. A. Russo, J. Leitão, C. Gama, J. Ferreira, and A. Monteiro, "Shipping emissions over europe: A state-of-the-art and comparative analysis," *Atmospheric Environment*, vol. 177, pp. 187–194, 3 2018.

[7] K. Cullinane and S. Cullinane, "Atmospheric emissions from shipping: The need for regulation and approaches to compliance," *Transport Reviews*, vol. 33, pp. 377–401, 7 2013.

[8] J. C. Ruth and G. Stephanopoulos, "Synthetic fuels: what are they and where do they come from?," *Current Opinion in Biotechnology*, vol. 81, p. 102919, 2023.

[9] C. J. McKinlay, S. R. Turnock, D. A. Hudson, and P. Manias, "Hydrogen as a deep sea shipping fuel: Modelling the volume requirements," *International Journal of Hydrogen Energy*, vol. 69, pp. 863–873, 6 2024.

[10] C. Raucci, J. Calleya, S. S. De, L. Fuente, and R. Pawling, "Hydrogen on board ship: A first analysis of key parameters and implications,"

[11] Y. Zhou, R. Li, Z. Lv, J. Liu, H. Zhou, and C. Xu, "Green hydrogen: A promising way to the carbon-free society," *Chinese Journal of Chemical Engineering*, vol. 43, pp. 2–13, 3 2022.

[12] H. Wang, P. Daoutidis, and Q. Zhang, "Ammonia-based green corridors for sustainable maritime transportation," *Digital Chemical Engineering*, vol. 6, 3 2023.

[13] C. J. McKinlay, S. Turnock, and D. Hudson, "A comparison of hydrogen and ammonia for future long distance shipping fuels," pp. 53–65, January 2020. Publisher Copyright: © 2020: The Royal Institution of Naval Architects.

[14] N. H. Prevljak, "World's first ammonia-ready vessel delivered." https://www.offshore-energy.biz/worlds-first-ammonia-ready-vessel-delivered/, 2022. Accessed: 2024-05-24.

[15] D. Ronen, "The effect of oil price on containership speed and fleet size," *Journal of the Operational Research Society*, vol. 62, pp. 211–216, 2011.

[16] D.-P. Song and J.-X. Dong, *Empty Container Repositioning*, pp. 163–208. Cham: Springer International Publishing, 2015.

[17] R. Epstein, A. Neely, A. Weintraub, F. Valenzuela, S. Hurtado, G. Gonzalez, A. Beiza, M. Naveas, F. Infante, F. Alarcon, G. Angulo, C. Berner, J. Catalan, C. Gonzalez, and D. Yung, "A strategic empty container logistics optimization in a major shipping company," *Interfaces*, vol. 42, pp. 5–16, 1 2012.

[18] D. Pacino, *Fast Generation of Container Vessel Stowage Plans using mixed integer programming for optimal master planning and constraint based local search for slot planning*. PhD thesis, IT University of Copenhagen, 2012.

[19] X. Wang and C. C. Teo, "Integrated hedging and network planning for container shipping's bunker fuel management," *Maritime Economics and Logistics*, vol. 15, pp. 172–196, 6 2013.

[20] O. Besbes and S. Savin, "Going bunkers: The joint route selection and refueling problem," *Manufacturing and Service Operations Management*, vol. 11, pp. 694–711, 9 2009.

[21] B. D. Brouer, J. Dirksen, D. Pisinger, C. E. Plum, and B. Vaaben, "The vessel schedule recovery problem (vsrp) - a mip model for handling disruptions in liner shipping," *European Journal of Operational Research*, vol. 224, pp. 362–374, 1 2013.

[22] L. A. Wolsey, *Integer Programming*. John Wiley & Sons, 1998.

[23] F. Oliveira, "Optimisation notes, a compilation of lecture notes from graduate-level optimisation courses."

[24] K. H. Borgwardt, *The simplex method: a probabilistic analysis*, vol. 1. Springer Science & Business Media, 2012.

[25] K. Miettinen, *Nonlinear Multiobjective Optimization*, vol. 12. Springer US, 1998.

[26] H. W. Hamacher, C. R. Pedersen, and S. Ruzika, "Finding representative systems for discrete bicriterion optimization problems," *Operations Research Letters*, vol. 35, pp. 336–344, 5 2007.

[27] M. Cococcioni, M. Pappalardo, and Y. D. Sergeyev, "Lexicographic multi-objective linear programming using grossone methodology: Theory and algorithm," *Applied Mathematics and Computation*, vol. 318, pp. 298–311, 2018.

[28] J. Liesiö, P. Mild, and A. Salo, "Preference programming for robust portfolio modeling and project selection," *European Journal of Operational Research*, vol. 181, pp. 1488–1505, 9 2007.

[29] Gurobi Optimization, "Gurobi documentation - Parameter descriptions." https://docs.gurobi.com/projects/optimizer/en/current/reference/parameters/descriptions.html#branchdir, 2024. Accessed: 2024-08-07.

[30] A. K. Jain, M. N. Murty, and P. J. Flynn, "Data clustering: A review," 2000.

[31] R. Weiss, T. Kanto, K. Kiviranta, and J. Kärki, "Large scale Industrial Power-to-X Production enabling Hydrogen Valleys: A Case Study of future Industrial Hydrogen Valley Opportunity in Finland," in *SDEWES2024 conference, Rome 8-12.09.2024*, 2024.

[32] BloombergNEF, "Wind and Solar Corporate PPA Prices Rise Up To 16.7% Across Europe." https://about.bnef.com/blog/wind-and-solar-corporate-ppa-prices-rise-up-to-16-7-across-europe/, 2022. Accessed: 2024-06-12.

[33] T. Lanshina, "Russia's wind energy market: Potential for new economy development," tech. rep., Friedrich-Ebert-Stiftung (FES), 2021.

[34] The Engineering ToolBox, "Fuels - Higher and Lower Calorific Values." https://www.engineeringtoolbox.com/fuels-higher-calorific-values-d_169.html, 2003. Accessed: 2024-06-12.

[35] S&P Global, "Interactive: Platts Ammonia price chart." https://www.spglobal.com/commodityinsights/en/market-insights/latest-news/energy-transition/051023-interactive-ammonia-price-chart-natural-gas-feedstock-europe-usgc-black-sea, 2024. Accessed: 2024-06-12.

[36] ExchangeRates, "US Dollar to Euro Spot Exchange Rates for 2024." https://www.exchangerates.org.uk/USD-EUR-spot-exchange-rates-history-2024.html, 2024. Accessed: 2024-06-12.

[37] The French National Institute of Statistics and Economic Studies, "International prices of imported raw materials - Heavy fuel oil (North west Europe)." https://www.insee.fr/en/statistiques/serie/010751333#Tableau, 2024. Accessed: 2024-08-12.

[38] T. C. Bond, S. J. Doherty, D. W. Fahey, P. M. Forster, T. Berntsen, B. J. Deangelo, M. G. Flanner, S. Ghan, B. Kärcher, D. Koch, S. Kinne, Y. Kondo,

P. K. Quinn, M. C. Sarofim, M. G. Schultz, M. Schulz, C. Venkataraman, H. Zhang, S. Zhang, N. Bellouin, S. K. Guttikunda, P. K. Hopke, M. Z. Jacobson, J. W. Kaiser, Z. Klimont, U. Lohmann, J. P. Schwarz, D. Shindell, T. Storelvmo, S. G. Warren, and C. S. Zender, "Bounding the role of black carbon in the climate system: A scientific assessment," *Journal of Geophysical Research Atmospheres*, vol. 118, pp. 5380–5552, 6 2013.

[39] The European Comission, "Commission delegated regulation (EU) 2023/1185 of 10 February 2023," *Official Journal of the European Union*, 2023.

[40] N. Rivedal, D. Slotvik, A. Mjelde, and Øyvind Endresen, "Ais analysis of nordic ship traffic," tech. rep., DNV, 2022.

[41] Gurobi Optimization, "Gurobi Python API." https://www.gurobi.com/features/gurobi-optimizer-delivers-rich-python-modeling-environment/, 2024. Accessed: 2024-08-29.

[42] Ember, "Daily European Union Emission Trading System (EU-ETS) carbon pricing from 2022 to 2024 (in euros per metric ton)." https://www.statista.com/statistics/1322214/carbon-prices-european-union-emission-trading-scheme/, 2024. Accessed: 2024-08-19.

[43] European Commission, "What is the EU ETS?." https://climate.ec.europa.eu/eu-action/eu-emissions-trading-system-eu-ets/what-eu-ets_en, 2024. Accessed: 2024-08-19.

[44] Ian Tiseo, "Forecast European Union Emissions Trading System (EU-ETS) average carbon allowance prices from 2024 to 2035." https://www.statista.com/statistics/1401657/forecast-average-carbon-price-eu-emissions-trading-system/#:~:text=European%20Union%20Emissions%20Trading%20System,dioxide%20(tCO%E2%82%82e)%20in%202024., 2024. Accessed: 2024-09-09.

A Synfuel price data

Sweden	
Component	**Price €/kg$_{H2}$**
Electrolyzer	1.03
H_2 Pipeline	0.48
El. transmission	0.21
Wind PPA	2.14
ELSPOT purchase	0.19
ELSPOT sales	-0.17
H_2 heat sales	-0.16
Other sales	-0.02
Total	**3.70**

Finland	
Component	**Price €/kg$_{H2}$**
Electrolyzer	1.03
H_2 Pipeline	0.48
El. transmission	0.21
Wind PPA	2.17
ELSPOT purchase	0.19
ELSPOT sales	-0.17
H_2 heat sales	-0.16
Other sales	-0.02
Total	**3.73**

Denmark	
Component	**Price €/kg$_{H2}$**
Electrolyzer	1.03
H_2 Pipeline	0.48
El. transmission	0.21
Wind PPA	2.48
ELSPOT purchase	0.19
ELSPOT sales	-0.17
H_2 heat sales	-0.16
Other sales	-0.02
Total	**4.04**

Poland	
Component	**Price €/kg$_{H2}$**
Electrolyzer	1.03
H_2 Pipeline	0.48
El. transmission	0.21
Wind PPA	3.41
ELSPOT purchase	0.19
ELSPOT sales	-0.17
H_2 heat sales	-0.16
Other sales	-0.02
Total	**4.97**

Germany	
Component	**Price €/kg$_{H2}$**
Electrolyzer	1.03
H_2 Pipeline	0.48
El. transmission	0.21
Wind PPA	3.47
ELSPOT purchase	0.19
ELSPOT sales	-0.17
H_2 heat sales	-0.16
Other sales	-0.02
Total	**5.03**

The Baltic countries	
Component	**Price €/kg$_{H2}$**
Electrolyzer	1.03
H_2 Pipeline	0.48
El. transmission	0.21
Wind PPA	4.19
ELSPOT purchase	0.19
ELSPOT sales	-0.17
H_2 heat sales	-0.16
Other sales	-0.02
Total	**5.75**

Russia	
Component	**Price €/kg$_{H2}$**
Electrolyzer	1.03
H_2 Pipeline	0.48
El. transmission	0.21
Wind PPA	4.96
ELSPOT purchase	0.19
ELSPOT sales	-0.17
H_2 heat sales	-0.16
Other sales	-0.02
Total	**6.52**

Table A1: Detailed price breakdown of the cost of hydrogen in nine countries [31].

B Sensitivity analysis solutions

B.1 10% increase in cost of hydrogen

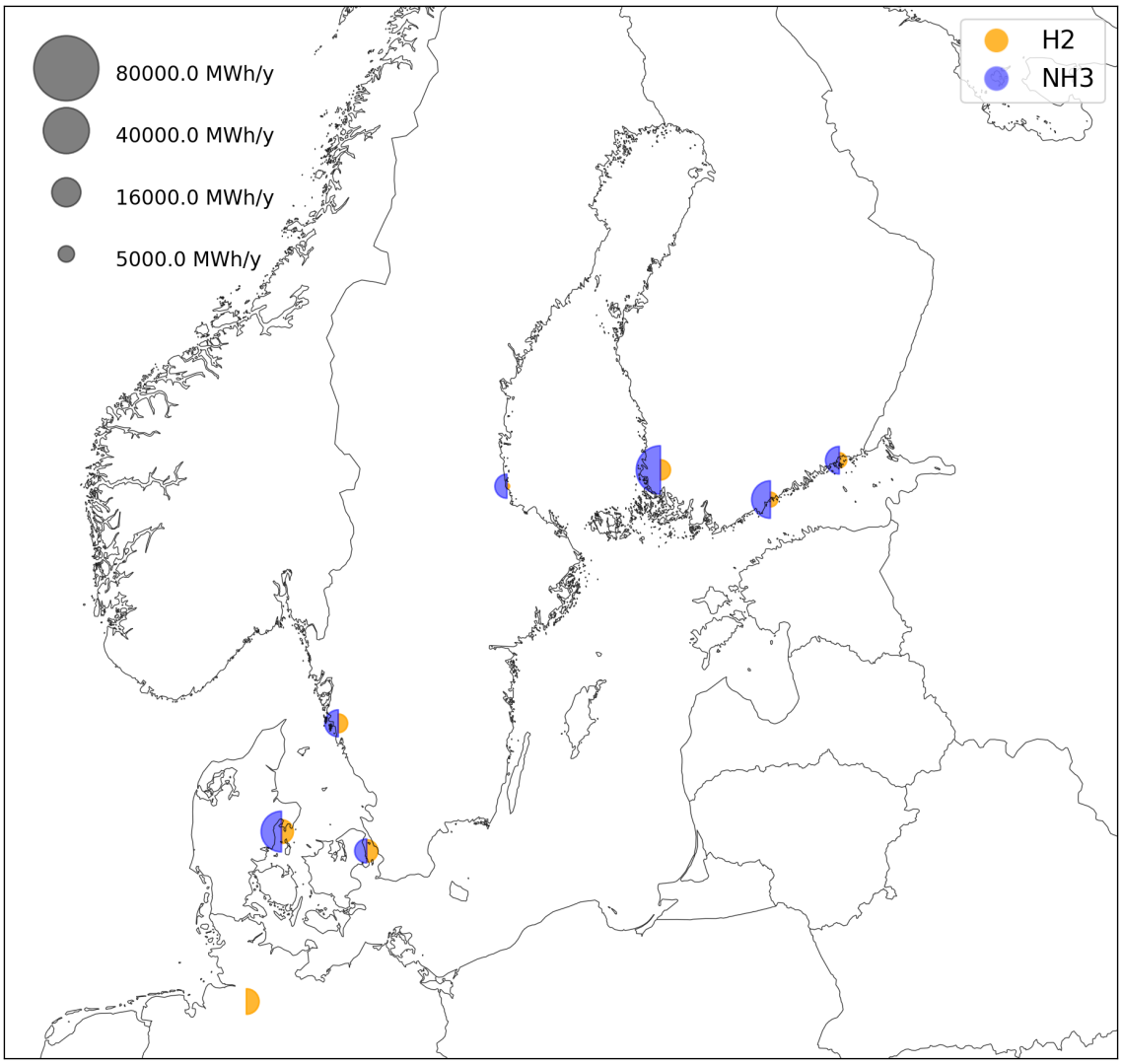

Figure B1: Production amounts for the most expensive Pareto optimal solution with a 10% increase in the cost of hydrogen.

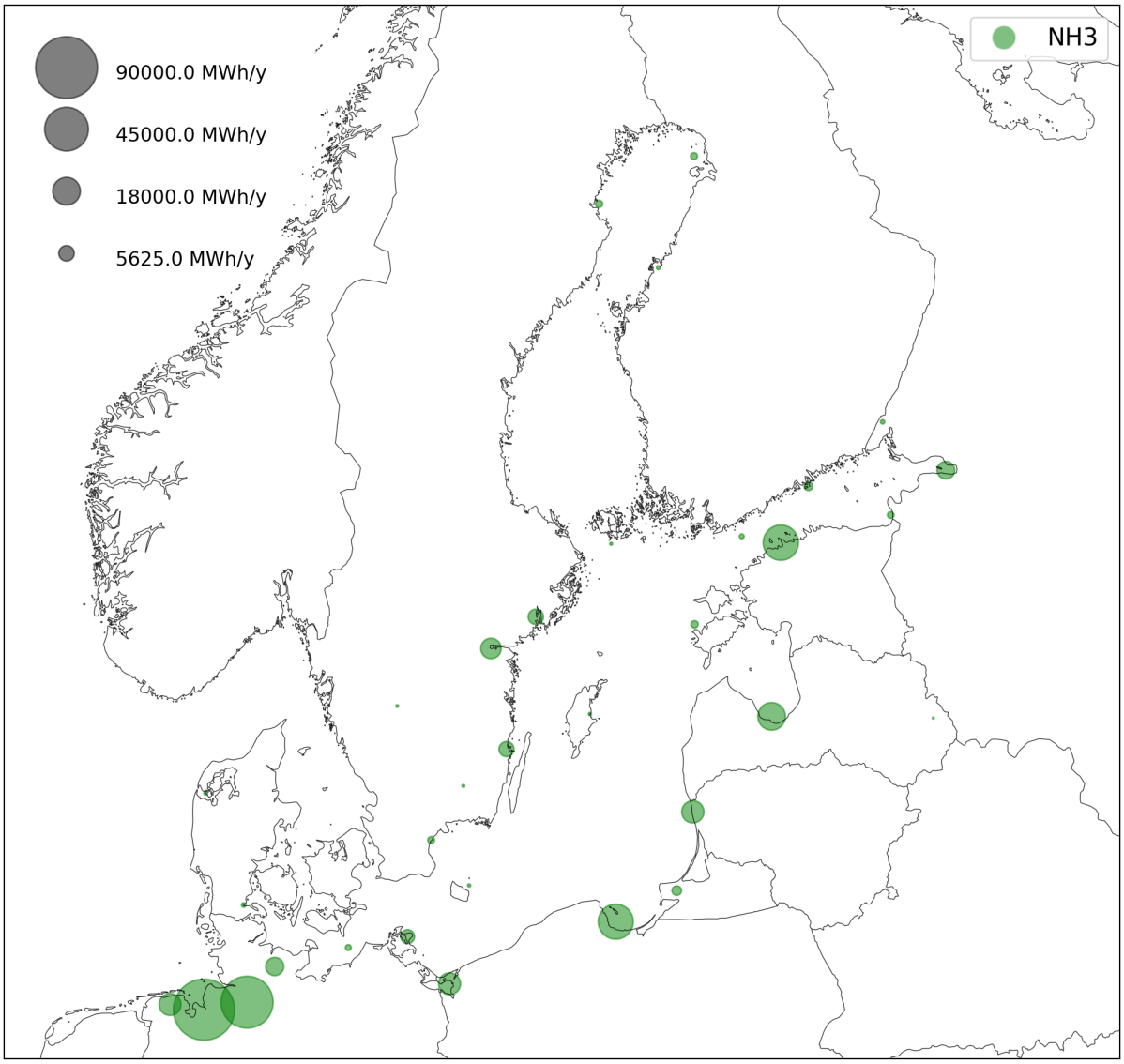

Figure B2: Purchase amounts for the most expensive Pareto optimal solution with a 10% increase in the cost of hydrogen.

B.2 10% decrease in cost of hydrogen

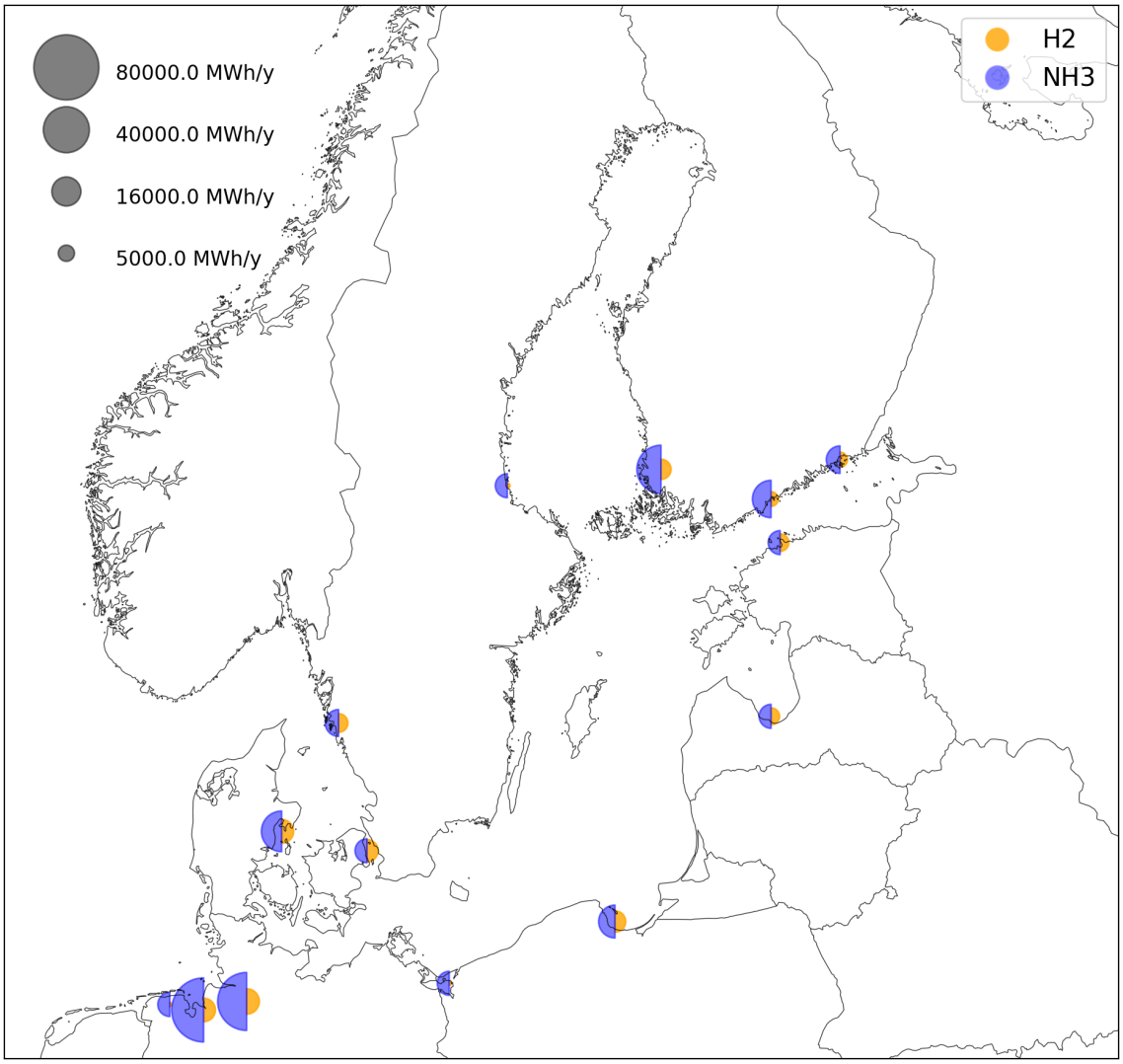

Figure B3: Production amounts for the most expensive Pareto optimal solution with a 10% decrease in the cost of hydrogen.

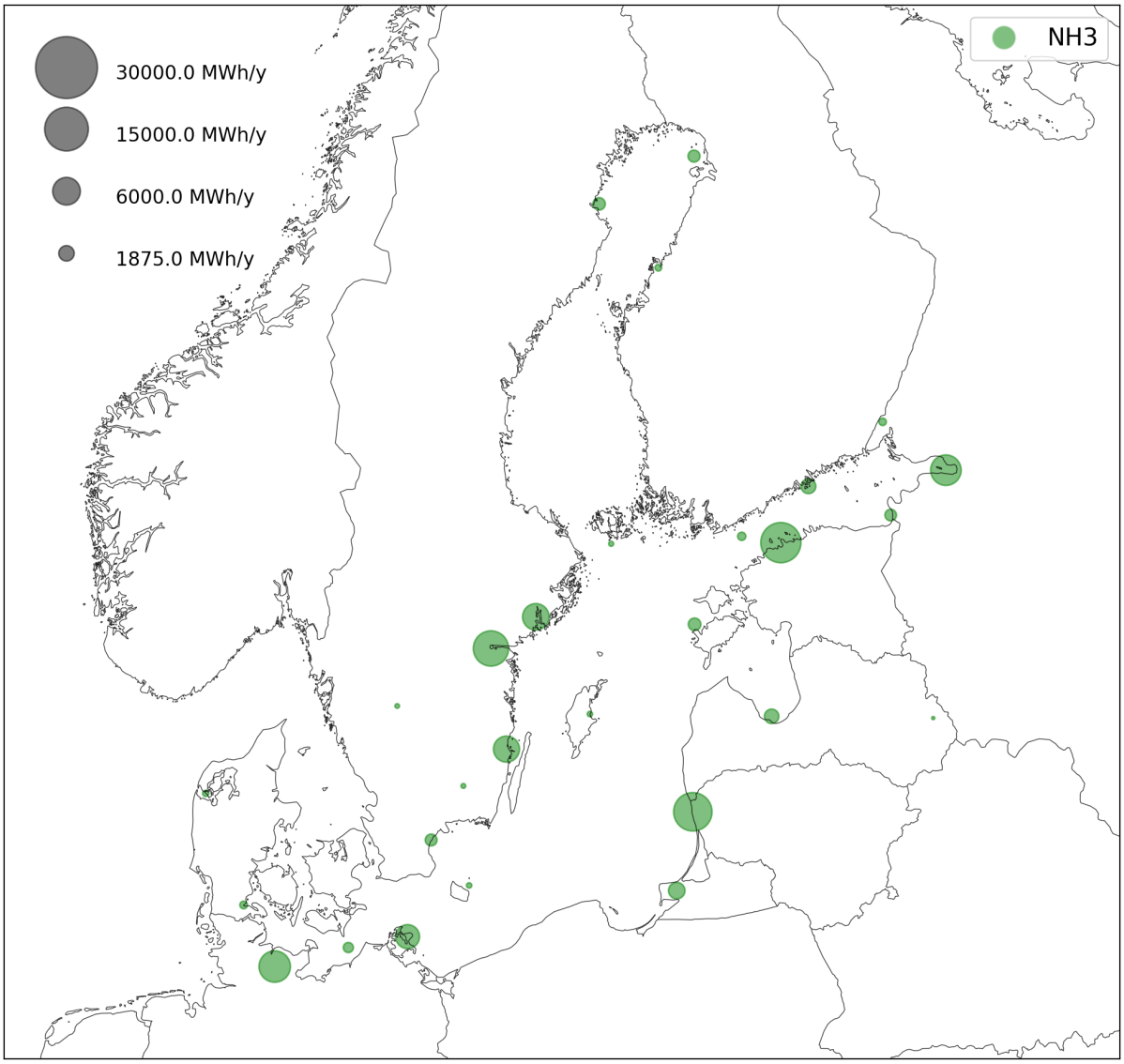

Figure B4: Purchase amounts for the most expensive Pareto optimal solution with a 10% decrease in the cost of hydrogen.

B.3 Minimum production rate of 5000 MWh/y

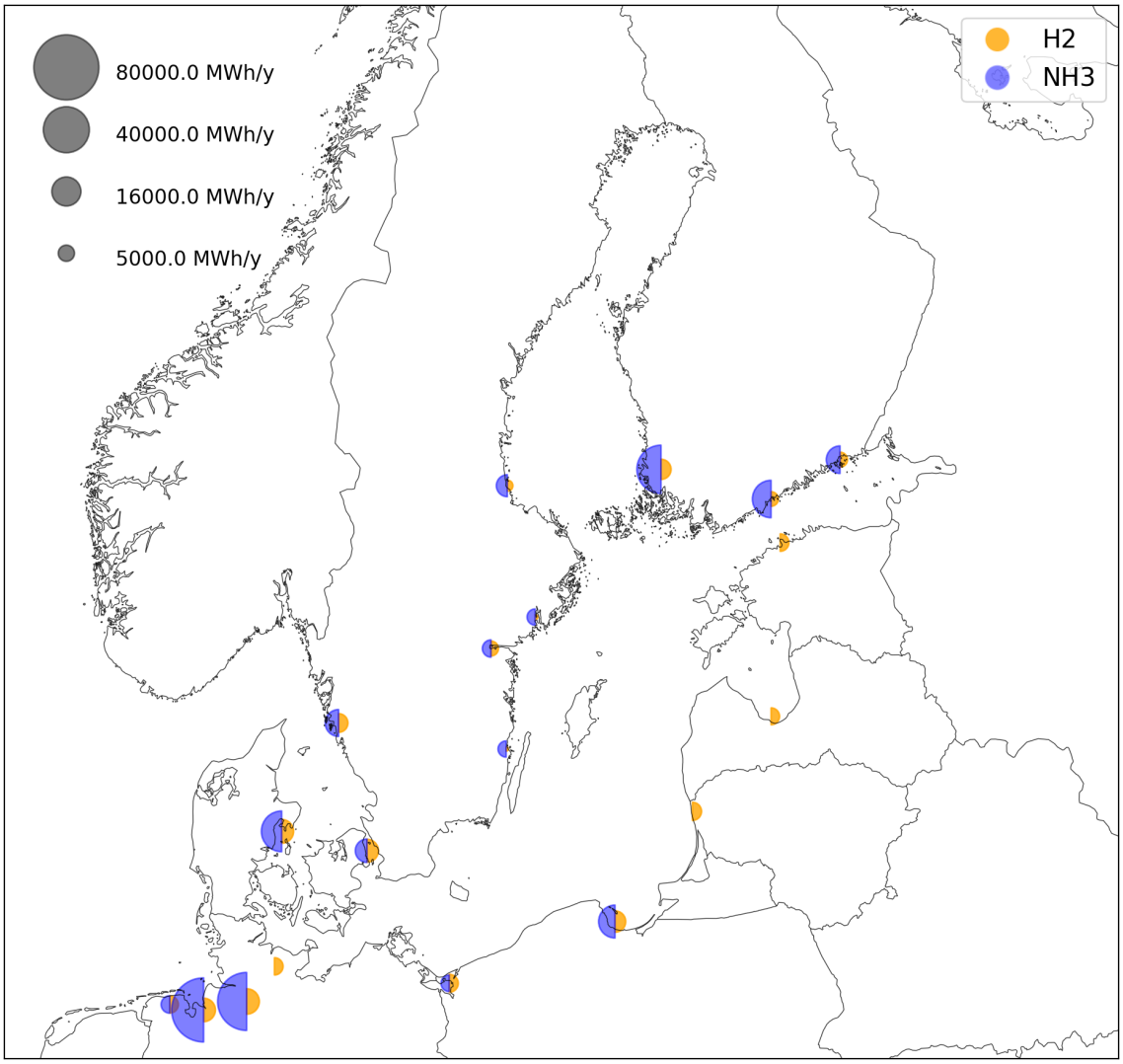

Figure B5: Production amounts for the most expensive Pareto optimal solution with a minimum production rate of 5000 MWh/y.

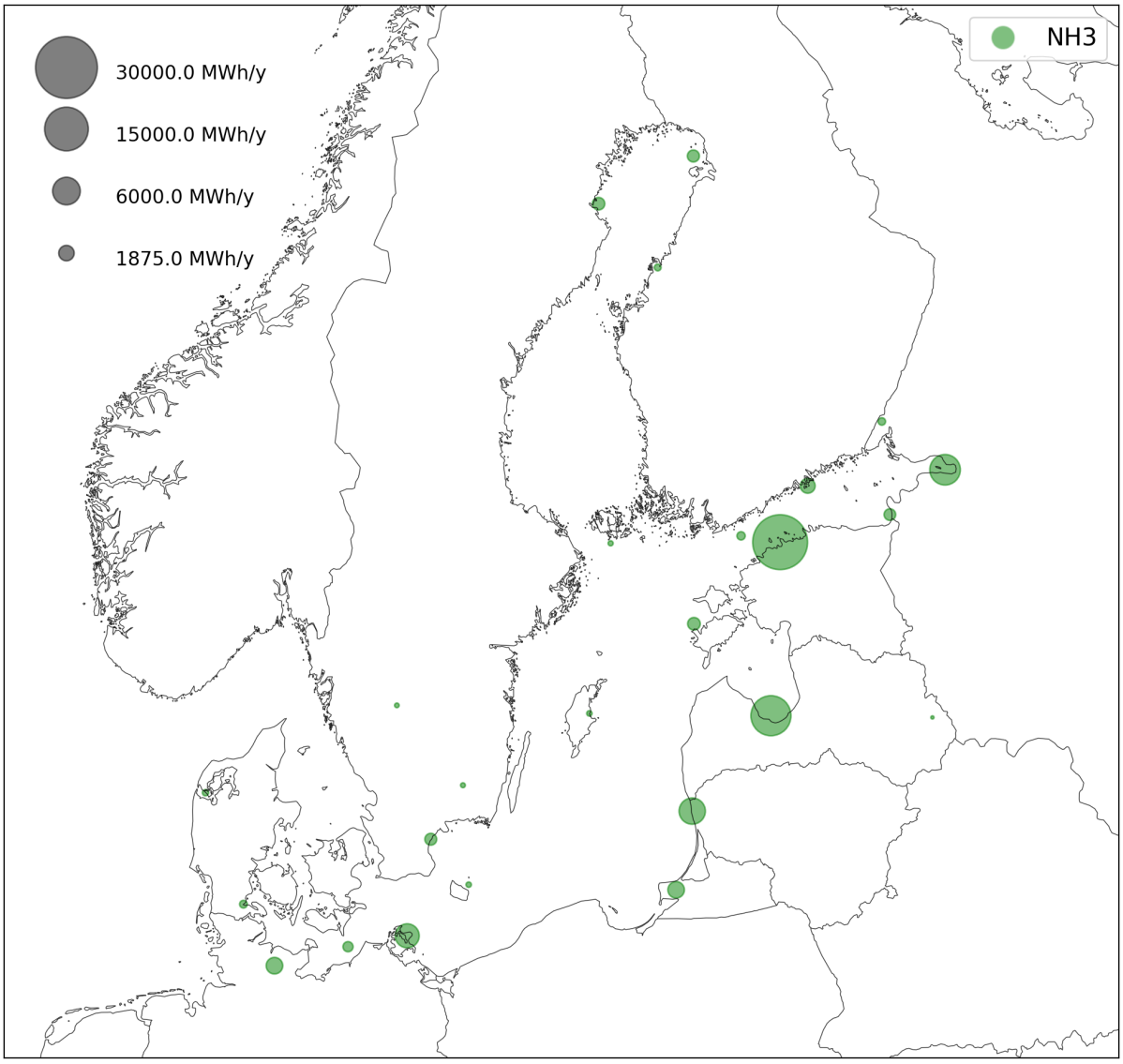

Figure B6: Purchase amounts for the most expensive Pareto optimal solution with a minimum production rate of 5000 MWh/y.

B.4 Minimum production rate of 1 MWh/y

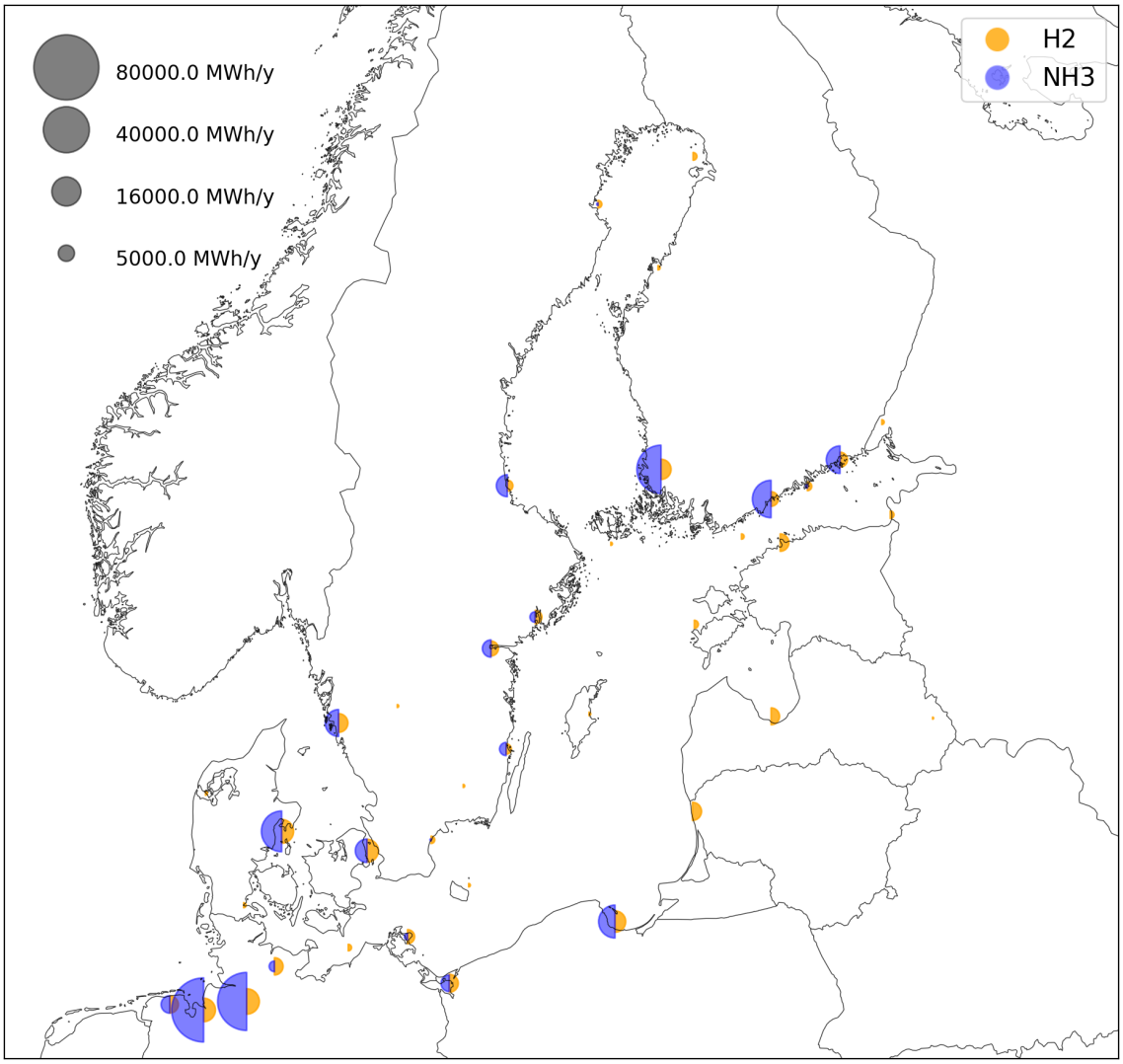

Figure B7: Production amounts for the most expensive Pareto optimal solution with a minimum production rate of 1 MWh/y.

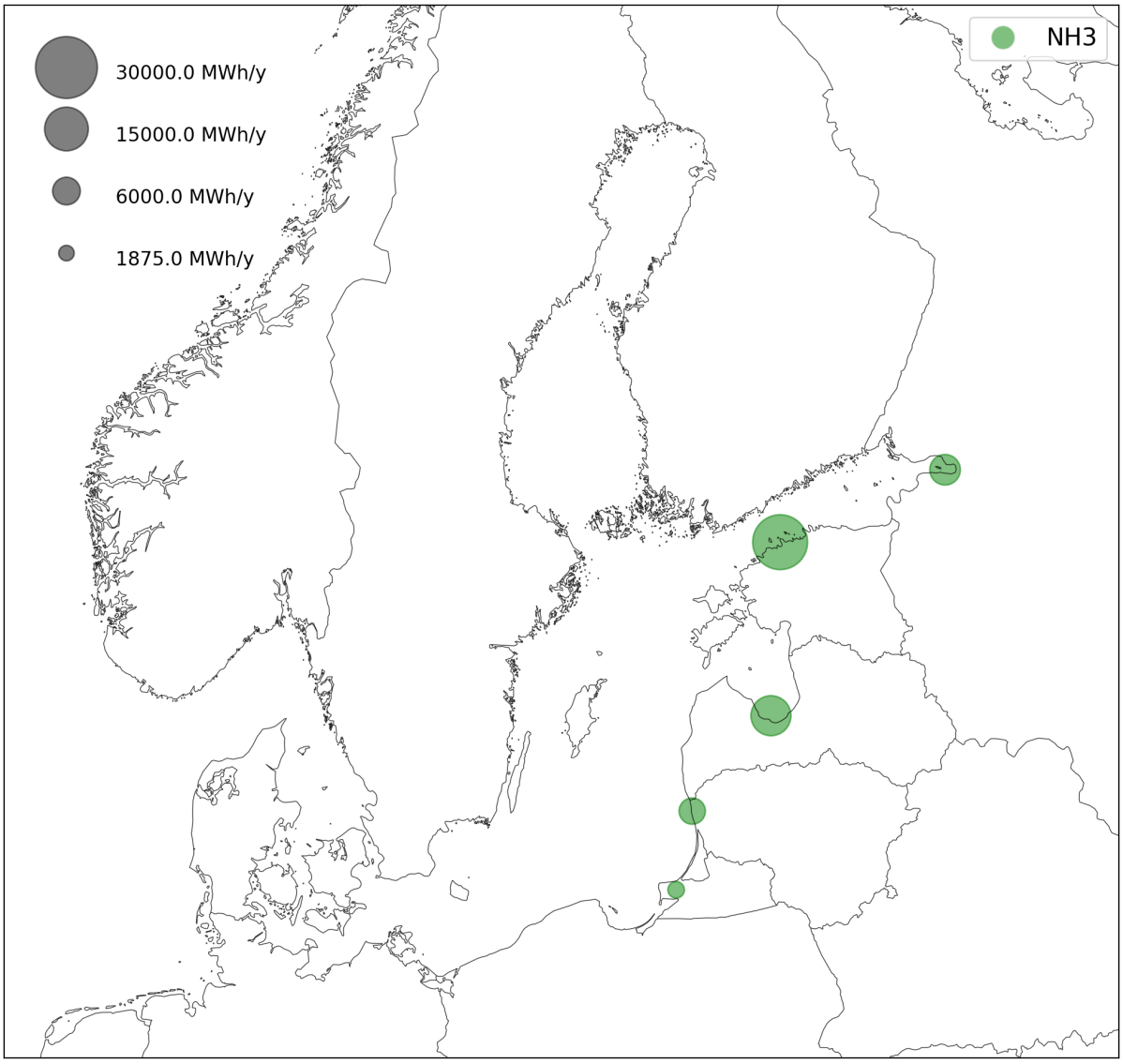

Figure B8: Purchase amounts for the most expensive Pareto optimal solution with a minimum production rate of 1 MWh/y.